

Rapidly-oscillating *TESS* A–F main sequence stars: are the roAp stars a distinct class?

L. A. Balona

South African Astronomical Observatory, P.O. Box 9, Observatory, Cape Town, South Africa

Accepted Received ...

ABSTRACT

From sector 1–44 *TESS* observations, 19 new roAp stars, 103 ostensibly non-peculiar stars with roAp-like frequencies and 617 δ Scuti stars with independent frequencies typical of roAp stars were found. Examination of all chemically peculiar stars observed by *TESS* resulted in the discovery of 199 Ap stars which pulsate as δ Sct or γ Dor variables. The fraction of pulsating Ap stars is the same as the fraction of pulsating chemically normal stars. There is no distinct separation in frequency or radial order between chemically peculiar δ Sct stars and roAp stars. In fact, all the features which originally distinguished roAp from δ Sct stars in the past have disappeared. There is no reason to assume that the high frequencies in roAp stars are driven by a different mechanism from the high frequencies in chemically normal stars. However, chemically peculiar stars are far more likely to pulsate with high frequencies. The term “roAp” should be dropped: all roAp stars are normal δ Scuti stars.

Key words: stars:oscillations; stars: chemically peculiar

1 INTRODUCTION

The peculiar Ap and Fp stars have strong, approximately dipolar, kilogauss global magnetic fields with axes which are generally tilted with respect to the rotation axes. They have inhomogeneous surface abundances and brightness, leading to rotational light modulation (the oblique rotator model [Stibbs 1950](#)). Their spectra have unusually strong lines of some ionized metals (e.g., Sr, Cr) and rare earth elements. The chemical peculiarities, which are confined to the outer layers, are thought to be a result of radiative acceleration, gravitational settling and diffusion.

The rapidly-oscillating Ap (roAp) stars are Ap/Fp stars which pulsate in a limited high-frequency range, typically above 60 d^{-1} ([Kurtz 1978, 1982](#)). When roAp stars were first discovered, the highest frequencies then detected among the δ Scuti stars were around 50 d^{-1} . These frequencies could be understood by the operation of the opacity driven κ mechanism in the HeII partial ionization zone ([Cox 1963](#)). The higher frequencies seen in roAp stars, however, could not be reproduced by models and seemed to require a new driving mechanism. For this reason, it seemed appropriate to make a distinction between δ Sct and roAp stars.

An additional reason why roAp stars were thought to be distinct from δ Sct stars is that high frequencies only seemed to occur among the chemically peculiar Ap stars. Furthermore, while δ Sct stars pulsate in a broad range of frequencies, the roAp stars pulsate with just a single high frequency or else with multiple closely-spaced high frequen-

cies. Another important difference is that in some roAp stars the frequency peaks are split by an exact multiple of the rotation frequency, something which is never seen in δ Sct stars. This can be understood by the oblique pulsator model ([Kurtz 1982; Kurtz & Shibahashi 1986](#)), in which the pulsation axis is tilted with respect to the rotational axis.

In conventional models, pulsational driving due to the κ mechanism acting in the H/He I partial ionization zone is almost enough to overcome damping in the rest of the star. This led [Balmforth et al. \(2001\)](#) to suggest that suppression of convection by a vertical magnetic field might be sufficient to reduce damping, resulting in driving of high-frequency pulsations confined to the region around the magnetic poles (see also [Cunha 2002, Cunha et al. 2013](#)). This new model seem to finally solve the problem of pulsational driving in roAp stars and explained why a strong magnetic field is required for the pulsations to occur. Since pulsational driving occurs only at the poles, the model neatly justifies why only axisymmetric modes are seen and the oblique pulsator model.

Further attempts to understand high-frequency pulsations in δ Sct stars were made by [Antoci et al. \(2014\)](#) who highlighted the role of turbulent pressure in the envelope convective zone. It was found that high frequencies could be excited in certain regions of the H–R diagram. Turbulent pressure is also considered as a possible mechanism in driving pulsations in Am stars ([Smalley et al. 2017](#)). The most comprehensive recent modelling of pulsations in δ Sct stars is that of [Xiong et al. \(2016\)](#), which also involves turbulent

pressure. The models predict high frequencies in a limited region of the H–R diagram.

Observations from the *Kepler* mission were the first to challenge the perception that pulsations in the δ Sct stars are fully understood. The models are unable to reproduce the low frequencies (i.e. below 5 d^{-1}) which are ubiquitous in δ Sct stars even at the highest effective temperatures (Balona 2014). Neither can they reproduce the fact that both γ Dor and δ Sct stars co-exist in the same effective temperature and luminosity region (Balona 2018). Another problem is that less than half of the stars in the δ Sct instability region seem to pulsate (Balona 2018).

TESS observations have also shown that high frequencies are not unique to roAp stars. Some δ Sct stars have independent frequency peaks extending into the roAp frequency range (Balona et al. 2019; Bedding et al. 2020). In this paper we present a list of 617 δ Sct stars with independent frequencies higher than 60 d^{-1} . These are chemically normal stars, showing that high frequencies are not confined to chemically peculiar stars. This invalidates the need for a special driving mechanism involving strong magnetic fields and suppression of convection at the poles (Balmforth et al. 2001).

Furthermore, many ostensibly normal A–F stars pulsate in isolated high frequencies or tight high-frequency groups just as in roAp stars (Cunha et al. 2019; Balona et al. 2019). Many of these have turned out to be chemically peculiar (Holdsworth et al. 2021), but this may not be true for all stars. In this paper we present more than 100 additional chemically normal stars with frequencies and frequency distributions that cannot be distinguished from roAp stars.

In this paper we also present the results of a survey of 1978 *TESS* Ap stars and the discovery that 199 are δ Sct or γ Dor stars. The idea that Ap stars do not pulsate is not correct. These new discoveries show that all the characteristics separating roAp stars from δ Sct stars are no longer applicable. It is clear that whatever mechanism drives high frequencies in normal stars must surely drive the high frequencies in “roAp” stars as well. The equally-spaced frequencies seen in some roAp stars are not seen in normal δ Sct stars. This is due to the action of a strong magnetic field on the atmospheric structure and does not require a separate pulsation mechanism.

The aim of this paper is to present new discoveries of “roAp” stars and non-peculiar roAp-like pulsators as well as a survey of pulsation in chemically peculiar stars. Using these results, it is argued that a suitable definition of the roAp class does not exist. Furthermore, it is argued that there is no criterion, other than a purely arbitrary frequency criterion, which can distinguish roAp stars from chemically peculiar or chemically normal δ Sct stars. It is concluded that the roAp classification is no longer a helpful guide to understanding pulsations in A–F stars and that the name “roAp” is misleading and should be abandoned.

2 THE DATA AND STELLAR PARAMETERS

The *TESS* photometric survey consists of continuous wide-band photometry of 13 sectors per celestial hemisphere. Each sector is observed continuously for about 27 days with 2-min cadence. Stars near the ecliptic equator are only ob-

served for one sector. Stars in the circular regions nearer the poles overlap so that, at the ecliptic poles, stars are observed continuously for about 100 days. The light curves are corrected for time-correlated instrumental signatures using pre-search data conditioning (PDC, Jenkins et al. 2016). The data used here are the full PDC light curves from sectors 1–44.

It should be noted that the *TESS* pixel size is 21×21 arcsec, which is roughly the size of the aperture used in ground-based photoelectric photometry. There is a possibility of contamination due to other stars in the same aperture. However, the stars discussed here are bright, mostly in the range 8–10 mag. The chances of contamination by another star of comparable brightness is quite remote. Contamination by a binary companion of comparable luminosity would be impossible to verify.

The most important step in any survey of this nature is to determine the variability type of each star. Automated classification is a relatively simple task, but without visual examination of the light curves and periodograms, there is no possibility of discovering anything new. For example, rotational modulation and flares in A stars would not have been noticed (Balona 2013). For this reason, visual inspection of the data is essential for further progress.

Using the SIMBAD database (Wenger et al. 2000), a master catalogue of about 684 000 stars brighter than magnitude 12.5 and with spectral types earlier than G0 was created. The catalogue includes the variability class if available, the effective temperature, luminosity, rotation period, spectral type and other useful parameters. The spectral type is important for ascertaining the variability class. It is also particularly useful because photometric effective temperature estimates are unreliable for B stars unless measurements in the U band are used (which is seldom the case). For example, the effective temperatures of B stars listed in the *Kepler* or *TESS* catalogues are not reliable. The master catalogue is not restricted to stars observed by *Kepler* or *TESS*.

As each *TESS* sector is released, stars in the bulk download file are matched with stars in the master catalogue and downloaded. The light curve from the FITS file is extracted automatically and stored in a database. If the star is already in the database, the additional data is appended to the existing light curve. Periodograms and extracted frequencies are calculated and form part of the database. Usually there are about 1000–2000 unclassified stars for each *TESS* release. Software tools (developed by the author) allow the periodogram and light curve to be displayed. Tools for smoothing the light curve, identifying harmonics and other useful functions are also included.

By visual inspection of the light curve and periodogram, the author has assigned a variability class to each star. In the few cases where a variability class is already known, there is good agreement. The task of visually classifying these stars typically takes two days. Changes are sometimes made to previously classified stars as more data become available. After each data release, the master catalogue is updated with the new classifications. The author has classified over 100 000 stars hotter than about 6000 K observed by *TESS* and *Kepler* in this way.

The variability classification follows that of the *General Catalogue of Variable Stars* (GCVS, Samus et al. 2017). A/F stars with rotational light modulation due to chemical

abundance spots (Ap stars) are classified as α^2 CVn (ACV) variables. Among the B stars these are known as SX Ari (SXARI) variables.

A new ROT class has been added to describe any star, not known to be chemically peculiar, in which the variability is suspected to be due to rotation. The criterion for ROT requires the presence of just a single, isolated frequency peak below 4d^{-1} or a peak and its harmonic. It is not always possible to distinguish rotation from binary effects, but to minimize such contamination, the ROT class is restricted to amplitudes below 10 millimag. The β Cep, SPB, Maia, δ Sct and γ Dor variables are typically multiperiodic and easily distinguished from the ROT stars.

A question arises as to what variability type must be assigned to a star which would be classified as roAp on the basis of the frequencies, but where the spectral type does not indicate chemical peculiarity. One could simply classify the star as a δ Sct. But what if the spectral type is incorrect and the star is indeed an Ap star? In that case one would lose the opportunity of detecting a new roAp variable. In these circumstances it is obviously important to make a note of these stars in some way. The solution that is adopted here is to label such stars as “roA” (ROA). This does not imply a new class of stellar variability, of course.

A separate catalogue was created containing individual T_{eff} measurements and literature references for as many as possible of the 684 000 stars in the master catalogue. This effective temperature catalogue presently contains over 185 000 individual T_{eff} measurements of about 101 500 stars, over and above the effective temperatures from the *Kepler* and *TESS* catalogues. The PASTEL catalogue (Soubiran et al. 2016) provided a very useful starting point for this compilation. Subsequent entries were made by searching the SIMBAD database.

For each entry in the effective temperature catalogue, the method used to derive T_{eff} was noted and assigned an index, t . If T_{eff} is derived from fitting a model atmosphere to the stellar spectrum, $t = 1$. If it is estimated from Strömgren, Geneva or other narrow-band photometry, $t = 2$. If T_{eff} is from the spectral energy distribution or similar method, $t = 3$. If it is from the *Kepler* or *TESS* catalogues $t = 4$. If it is estimated from the spectral type, $t = 5$. The adopted value of T_{eff} is the average of all the values with lowest t . Measurements with higher t values are ignored. From time to time, the master catalogue is updated with the adopted T_{eff} .

Photometric effective temperatures for Ap stars are unreliable because of line blanketing due to the spectral peculiarities. For this reason, it is best to use spectroscopic measurements ($t = 1$) whenever possible. Table 1 lists all individual T_{eff} values and references used to determine the adopted T_{eff} for stars listed in the Appendix. The table contains 574 entries for all 443 stars mentioned in this paper. For these stars, a thorough literature search was made to ensure that all available measurements are included.

Spectral types are mostly from the catalogue of Skiff (2014) supplemented by later publications when required. The calibration of Pecaut & Mamajek (2013) was used to estimate T_{eff} as a function of spectral type for those stars where the spectral type is the only available method of estimating T_{eff} ($t = 5$).

The stellar luminosity listed in the tables was estimated

Table 1. Catalogue of effective temperatures, T_{eff} , index, t , and literature reference. The full table is available in electronic form.

| TIC | t | T_{eff} | Ref |
|---------|-----|------------------|---------------------|
| 2849758 | 4 | 9033 | 2018AJ...156..102S |
| 3373254 | 5 | 7790 | 2013ApJS..208...9P |
| 3542929 | 5 | 8500 | 2013ApJS..208...9P |
| 3814749 | 2 | 7861 | 2020A&A...638A..76Q |
| 3814749 | 2 | 8029 | 2019A&A...628A..94A |
| 4463975 | 1 | 7629 | 2020ApJS..247...28H |
| 5370150 | 2 | 6927 | 2019A&A...628A..94A |

from *Gaia* EDR3 parallaxes (Gaia Collaboration et al. 2016, 2018) in conjunction with reddening obtained from a three-dimensional map by Gontcharov (2017) using the bolometric correction calibration by Pecaut & Mamajek (2013). From the error in the *Gaia* EDR3 parallax, the typical standard deviation in $\log(L/L_{\odot})$ is estimated to be about 0.05 dex, allowing for standard deviations of 0.01 mag in the apparent magnitude, 0.10 mag in visual extinction and 0.02 mag in the bolometric correction in addition to the parallax error. However, comparison between EDR3 and DR2 releases of the *Gaia* parallaxes suggests that the real error in luminosity is probably closer to 0.07 dex.

3 COMPARISON BETWEEN CHEMICALLY PECULIAR δ SCT AND ROAP STARS

We need to ask what characteristics are traditionally used in classifying a star as roAp. The general view is that roAp stars are simply Ap stars with high frequencies, but there is no consensus on the meaning of “high frequencies”. The lowest frequency in the group of recognized roAp stars (as listed in Smalley et al. 2015) is 61d^{-1} . It is reasonable to suppose, then, that “high frequencies” means any frequency higher than about 60d^{-1} .

Definition of a variability group should be based on physical considerations and not arbitrary choices. However, since no other definition has been proposed, it will be assumed that a star is roAp only if the pulsation frequency is higher than the hard limit of 60d^{-1} . Low-frequency peaks which can be attributed to rotation are often detected as well. Lower frequencies typical of γ Dor or δ Sct stars may co-exist with the high frequencies, in which case the star is given a hybrid classification, e.g. DSCT+ROAP.

Note that recently Holdsworth et al. (2021) admitted TIC 356088697, which has a single pulsation mode at 55.8d^{-1} , to the list of roAp stars. There is no real reason to query the lowering of the frequency limit, because there is no theory which provides a guide on the supposed frequency range in which roAp stars may pulsate. In fact, one might as well use any limit that feels right. This is clearly not a satisfactory situation.

Table A1 lists all known roAp stars, even those not observed by *TESS*. This is essentially the list in Smalley et al. (2015) supplemented by *TESS* discoveries by Cunha et al. (2019) and Balona et al. (2019) and, most recently, by Holdsworth et al. (2021). The sources of T_{eff} for these stars are listed in Table 1. The rotation periods in this and other tables are either those in the literature or updated by the author using the *TESS* light curves. The characteristic fre-

quency, ν , is the frequency of highest amplitude above 60 d^{-1} .

The Am (metallic-lined) stars are characterized by an under-abundance of Ca (and/or Sc) and/or an over-abundance of Fe and the iron-group elements. Unlike the Ap stars, the abundances of rare earth elements are normal and a global magnetic field is absent or very weak. The high metal abundance is thought to be a result of diffusion in the absence of a magnetic field (Michaud et al. 1976). As mentioned by Holdsworth et al. (2014), it is difficult to distinguish between Am and Ap stars at classification dispersion.

For this reason, and because Am stars are not known to pulsate with high frequencies, stars classified as Am are included in the tables as possibly mis-classified roAp stars. Rotational variables among Am stars are assigned the ROT class (not ACV). Some stars which are not known to be Ap, but which have been accepted in the literature as being roAp are also listed.

All known chemically peculiar stars observed by *TESS* were examined for pulsational variability. Quite a large number of δ Sct and γ Dor Ap stars were found (Table A2). These will be discussed separately below.

Fig. 1 shows the periodograms of a number of Ap δ Sct stars from Table A2 as well as roAp stars from Table A1. We note that there is no obvious frequency separation between stars which are classified as roAp, i.e. those with frequencies higher than 60 d^{-1} (right panel) and those of slightly lower frequencies (left panel), which we must presumably regard as Ap δ Sct stars. Note that the stars shown in the figure have single or isolated multiple high frequencies typical of roAp stars. The situation where a variability group is defined on the basis of an arbitrary frequency limit, but where no basis for such a limit exists, is clearly not satisfactory.

The main characteristic used to define roAp stars - that of high frequencies - can no longer be used. There is no frequency which marks an obvious lower limit to pulsations in Ap stars. Neither is there a discernible frequency gap between δ Sct and roAp classification. The argument that chemically peculiar stars do not pulsate cannot be used to justify the roAp class either.

4 NEW ROAP AND ROAP-LIKE STARS

Table A3 lists previously unreported *TESS* stars with effective temperatures $T_{\text{eff}} > 6000 \text{ K}$ in which at least one significant, independent frequency peak higher than 60 d^{-1} is present. The test for significance is based on the criterion that the peak amplitude must exceed the mean local noise level by a certain factor. It is not possible to directly calculate the false alarm probability in this way. The generally used criterion of $S/N > 4$ (Breger et al. 1993) is probably too optimistic (Baran et al. 2015; Baran & Koen 2021; Bowman & Michielsen 2021). Here we use the criterion $S/N > 4.7$, but of course there will always be uncertainty at low values of S/N .

Table A3 lists 19 known Ap stars with isolated high-frequency peaks or group of peaks higher than 60 d^{-1} which have not been previously reported. These would certainly be accepted as new stars of the roAp class. However, the majority of new pulsating stars in Table A3 are chemically normal. From this perspective, they are just δ Sct stars unless fur-

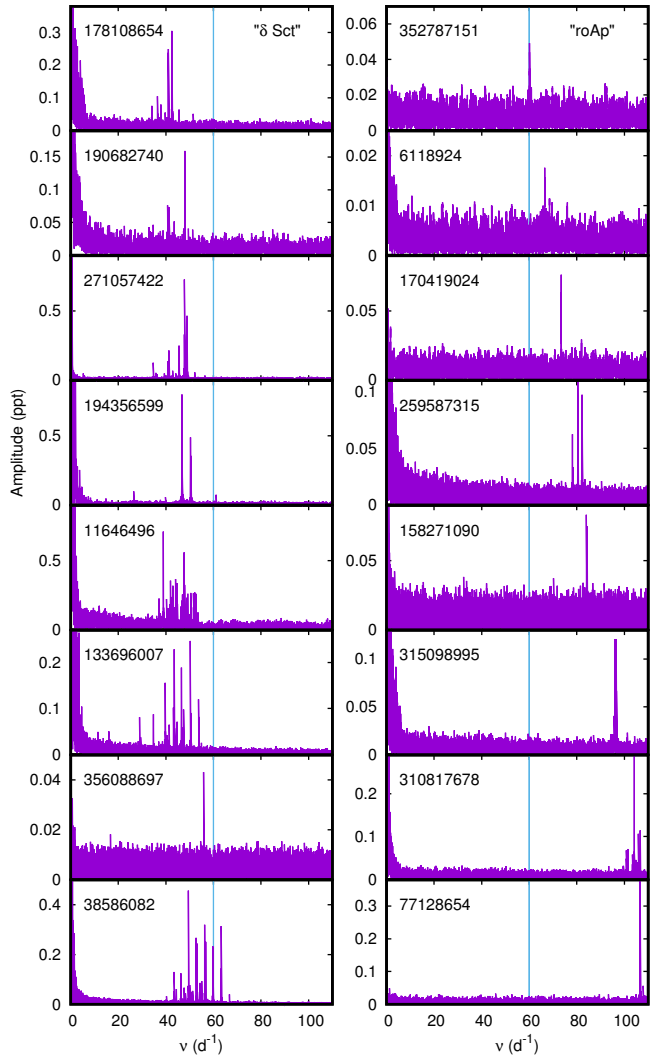


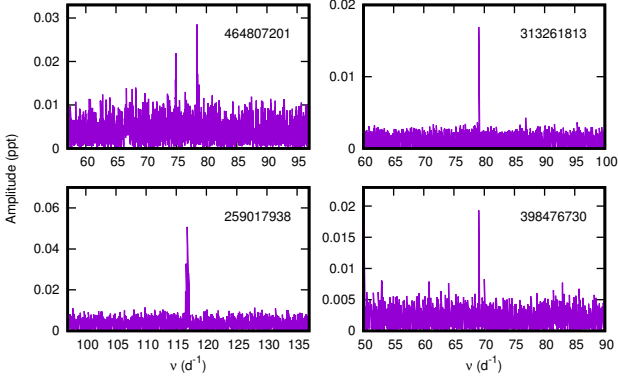
Figure 1. The periodograms of some Ap stars arranged in order of increasing frequency. The left panel shows what may be classified as δ Scuti variables while the right panel are all known roAp stars. As can be seen, there is no distinct separation between the two classes of Ap pulsating stars except for the artificial boundary at 60 d^{-1} (vertical line).

ther study shows that they are chemically peculiar. Labeling these roAp-like stars as “roAp” is not correct as there is no evidence that they are chemically peculiar. Classifying them as δ Sct would also not be correct because it is possible that some may turn out to be chemically peculiar. For this reason, the temporary label “roA” has been assigned to them. This does not signify a new class of variable star, but is simply a label to identify stars which cannot be properly classified until chemical peculiarity has been satisfactorily established or ruled out.

It would be expected that chemical peculiarities would be most easily detected in bright stars, yet the spectral classifications of many of the brightest roA stars do not mention chemical peculiarity. Four of these bright roA stars are listed in Table 2 and their periodograms shown in Fig. 2. As can be seen, these would certainly be classified as roAp stars. HD 119476 (TIC 313261813), for example, has been given

Table 2. Bright ROA stars discovered from *TESS* photometry.

| TIC | Name | Var. Type | V | Sp. Type |
|-----------|-----------|--------------|------|----------|
| 313261813 | HD 119476 | GDOR+ROT+ROA | 5.85 | A1.5V |
| 398476730 | HD 104125 | ROT+ROA | 6.76 | A2V |
| 464807201 | HD 29839 | ROA+ROT | 7.10 | A1V |
| 259017938 | HD 210684 | ROT+ROA+r | 7.37 | F0 |


Figure 2. Examples of bright stars, not known to be chemically peculiar, with high roAp-like frequencies.

spectral types in the range B9V–A2V by seven different authors (Skiff 2014) and in no case was chemical peculiarity identified.

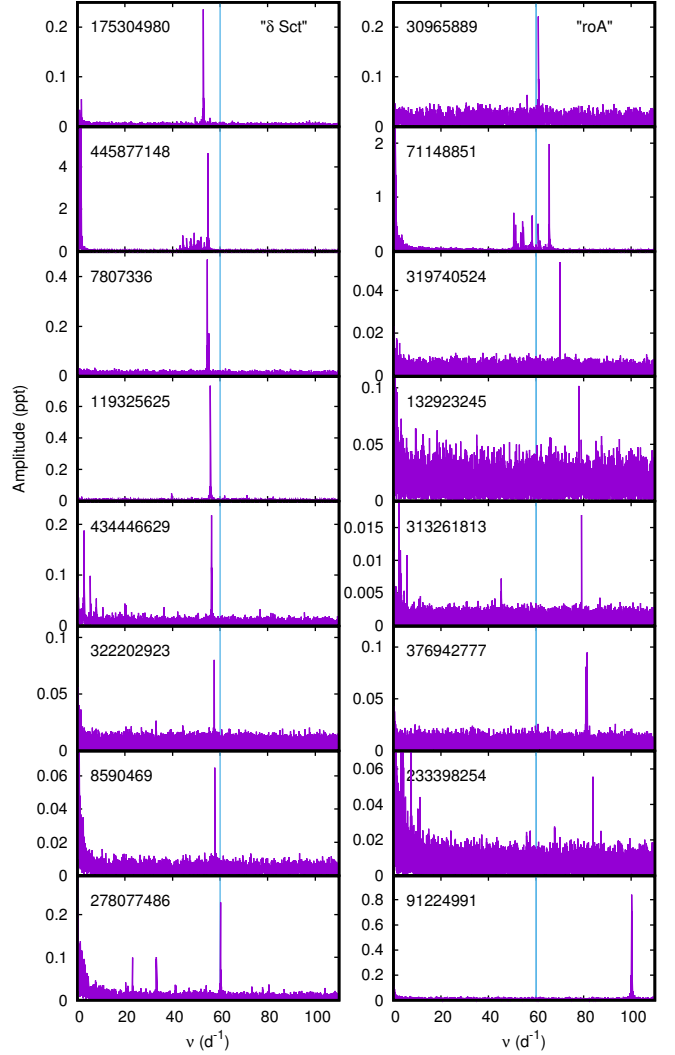
Fig. 3 shows periodograms of some ostensibly chemically normal roA stars arranged in order of increasing frequencies. We see that, as in the roAp stars, there is no separation between the roA and normal δ Scuti stars. What this figure also shows is that isolated frequency peaks, which are typical of roAp stars, are quite common among δ Sct stars as well (see Balona 2021b).

5 RADIAL ORDER AS A POSSIBLE DISCRIMINANT

It may perhaps be possible to discriminate between roAp stars and roAp-like δ Sct stars on the basis of pulsational radial order, as attempted in Balona et al. (2019). This is not likely to succeed because there is clearly a strong correlation between frequency and radial order. Furthermore, there is no physical basis why radial order should be important, but it is worth the attempt.

The radial order, n , associated with pulsation frequency for known roAp stars in Tables A1 was derived from the stellar parameters and pulsation models by Dziembowski (1977). Fig. 4 compares the radial order calculated for roAp stars (left panels) and for roA stars (right panels). The top panel shows the correlation between pulsation frequency and radial order. The scatter is due to stars in different stages of evolution. The middle panel shows n as a function of effective temperature. The bottom panel shows the pulsation frequency as a function effective temperature.

One might suppose, for example, that roAp pulsation might only occur above a certain radial order number. In that case the plot of radial order as a function of T_{eff} should show a hard boundary. As can be seen, this is not the case and the range in radial order is just as large as the range


Figure 3. The periodograms of some ostensibly chemically normal stars arranged in order of increasing frequency. The vertical line is the adopted limit of 60 d^{-1} . By analogy with the roAp stars, stars with at least one frequency higher than this limit are called “roA” stars, even though this distinction is purely arbitrary.

in frequency for both roAp and roA stars. Using the radial order offers no advantage over frequency as a means of distinguishing roAp/roA stars from δ Sct stars.

6 HYBRID δ SCT ROAP AND HIGH-FREQUENCY δ SCT STARS

Among the recognised roAp stars in Table A1, there are 10 δ Sct+roAp hybrids. A further three new δ Sct+roAp hybrids are listed in Table A3. It is, of course, possible that these stars are all multiple systems in which one star is δ Sct and the other a pure roAp star. This cannot be ruled out, but appears rather contrived. Recently, Murphy et al. (2020) have concluded that most of these δ Sct+roAp hybrids are not multiple stars.

There is a large number of chemically normal δ Sct variables with high frequencies. Whereas roAp and roA stars

Table 3. List of 617 new δ Sct stars with independent high frequencies exceeding 60 d^{-1} . The columns are the same as in Table A1. The full table is available in electronic form.

| TIC | Name | Var Type | ν (d^{-1}) | T_{eff} (K) | $\log \frac{L}{L_{\odot}}$ (dex) | P_{rot} (d) | Sp Type |
|---------|-----------|--------------|------------------------------|-------------------------|-------------------------------------|-------------------------|---------|
| 1221946 | HD 30461 | DSCT+ROA | 62.016 | 7671 | 1.03 | | A2/3II |
| 1404122 | HD 80750 | DSCT+ROA | 60.152 | 8981 | 1.26 | | A0V |
| 2004993 | HD 34113 | DSCT+ROT+ROA | 60.265 | 8885 | 1.31 | 7.143 | A0 |
| 3891160 | HD 99120 | DSCT+ROA | 61.420 | 8614 | 1.21 | | A1V |
| 4154746 | HD 294001 | DSCT+ROA | 61.945 | 8490 | 1.12 | | A2 |
| 4202325 | HD 35221 | DSCT+ROA | 71.942 | 8506 | 1.07 | | A2 |
| 4250763 | HD 35318 | DSCT+ROA | 78.658 | 9414 | 1.40 | | A0 |

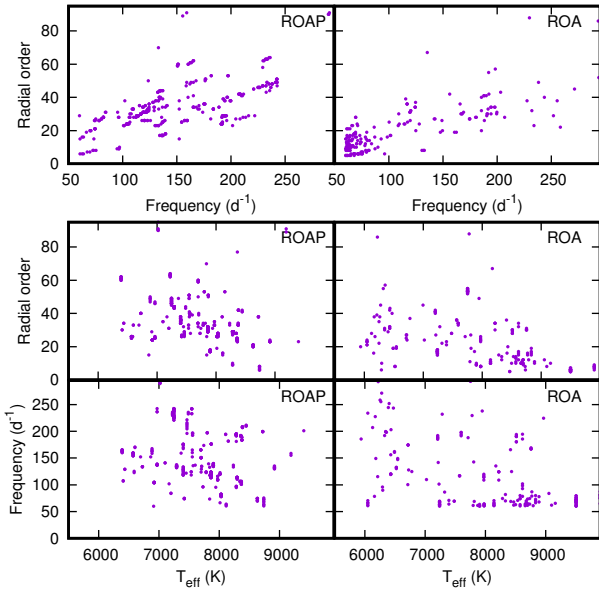


Figure 4. Top panel: the radial order, n , as a function of pulsation frequency. Middle panel: the radial order, n , as a function of effective temperature. Bottom panel: pulsation frequency as a function of effective temperature. The left panel shows stars recognised as roAp (Table A1). The right panel shows stars which have the same photometric characteristics as roAp stars but are not known to be chemically peculiar. These are presumably normal δ Sct stars, but here they are called roA stars because some might be misclassified Ap stars.

have only a few isolated high-frequency peaks, these high-frequency δ Sct stars have rich frequency spectra extending well into the roAp range. Most of the high frequencies are combinations and harmonics arising from non-linear interaction of low-frequency independent modes.

Independent frequencies may be determined by looking at all possible combinations of parent frequencies, ν_1 and ν_2 , such that $\nu = n_1\nu_1 + n_2\nu_2$, where n_1 and n_2 are positive or negative integers with $|n_1| \leq |n_{\text{max}}|$, $|n_2| \leq |n_{\text{max}}|$. The value of n_{max} should not be too large because for a sufficiently large value, almost any frequency can be described by a combination. It should also not be too low as to miss on a possible low-order interaction. As a compromise, $n_{\text{max}} = 7$ was chosen. In deciding whether a combination, ν , is significantly different from the observed frequency, ν_{obs} , the criterion $|\nu - \nu_{\text{obs}}| < 3\sigma$ was used, where σ is given by

$$\sigma^2 = \sigma_{\text{obs}}^2 + \sigma_1^2 + \sigma_2^2,$$

and σ_{obs} is the standard deviation of the observed frequency. The standard deviations of the parent frequencies are σ_1 and σ_2 .

There are at least 617 δ Sct stars with independent high frequencies in the roAp range. These are listed in Table 3. To distinguish them from other high-frequency δ Sct stars, they are labeled as δ Sct+roA. This is not meant to be a new class of variable, but just a convenient label.

It is not clear why δ Sct+roA stars should be driven by a different mechanism or how such stars are to be differentiated from δ Sct+roAp hybrids. In other words, chemically normal δ Sct stars with high frequencies can be considered to be in the same group as chemically peculiar δ Sct stars with high frequencies. There is no reason why the pulsation mechanism in these two groups should be different.

7 LOCATION OF STARS IN THE H-R DIAGRAM

High-frequency stellar pulsations are to be found in stars with high mean densities. As Fig. 5 shows, the δ Sct+roA or δ Sct+roAp stars are found close to the zero-age main sequence where the mean densities are the largest. One may expect stars with lower frequencies to be more evolved because they would be less dense and have larger radii. To show this, δ Sct with frequencies higher than 50 d^{-1} but not higher than 60 d^{-1} (labeled as DSCTHF in the figure), are, on average, slightly more evolved, as expected.

Most roAp and roA stars populate the cooler half of the δ Sct instability region. There are a significant number of roA stars cooler than the red edge of the δ Sct instability strip defined by the *Kepler* δ Sct stars. The pulsations in these cool roA stars cannot be mistaken for solar-like oscillations because the typical Gaussian envelope of peak amplitudes is not seen. Furthermore, the stars do not obey the scaling law for solar-like oscillations (Kjeldsen & Bedding 1995). However, there are indications that the δ Sct instability region defined by *TESS* stars is extended towards cooler stars compared to the *Kepler* instability region shown in Fig. 5. This may be a result of metallicity differences between the *Kepler* and *TESS* stars. Most likely these cool roA stars are simply δ Sct stars in which isolated high frequencies in the roAp range are selected.

8 Ap STARS WITH δ SCUTI PULSATIONS

Saio (2005) performed a non-adiabatic analysis of axisymmetric nonradial pulsations in the presence of a dipole mag-

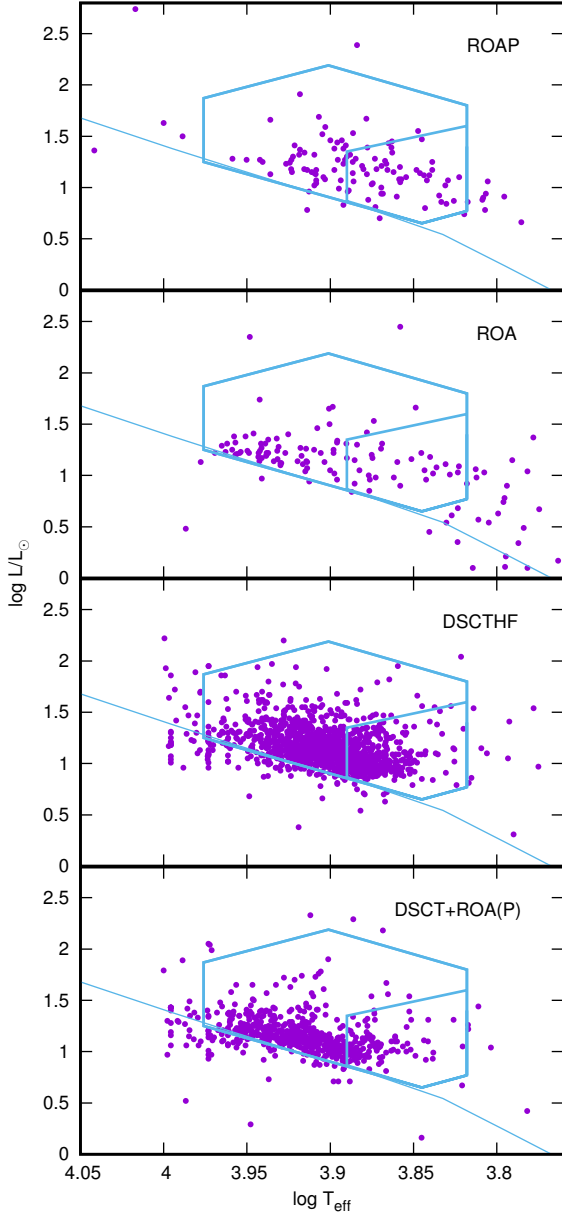


Figure 5. The top two panels show the locations of the roAp and roA stars in the theoretical H-R diagram. The third panel shows δ Sct stars with frequency peaks $50 < \nu < 60 \text{ d}^{-1}$ (high-frequency δ Sct stars, DSCTHF). The bottom panel shows δ Sct stars with at least one independent frequency $\nu > 60 \text{ d}^{-1}$. The solid line is the zero-age main sequence for solar abundance models by Bertelli et al. (2008). The polygons are the approximate areas where most δ Scuti and γ Dor stars are found (Balona 2018).

netic field for a model with $M = 1.9 M_{\odot}$ in which convection was suppressed in the stellar envelope. It was found that δ Sct pulsations are damped if the polar field strength is larger than about 1 kG. However, high-order p modes with frequencies corresponding to roAp stars driven by the κ mechanism in the H α ionization zone remain overstable, even in the presence of a strong magnetic field. This analysis suggests that roAp pulsations should not co-exist with δ Sct pulsations in Ap stars unless the magnetic field strength is lower than about 1 kG.

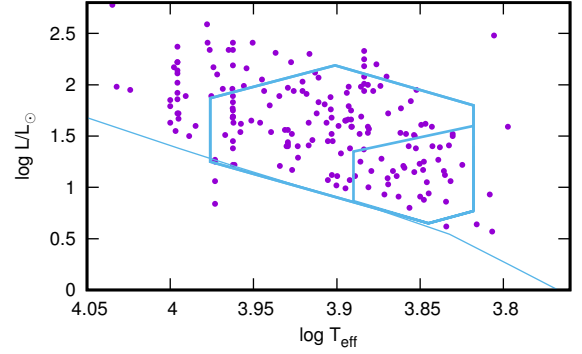


Figure 6. Location of chemically peculiar δ Sct stars of Table A2 in the theoretical H-R diagram.

More recent calculations by Murphy et al. (2020) indicate that the fundamental mode can be excited even in the presence of a magnetic field as strong as 4 kG, but high radial order g modes typical of γ Dor pulsations are strongly suppressed. If this prediction is correct, there should not be many Ap stars with low-frequency γ Dor pulsations. There are 199 Ap/Fp stars in which δ Sct or γ Dor pulsations are present (Table A2). Most of the Ap δ Sct stars have multiple low-frequency peaks indicative of high radial order g modes, suggesting a possible problem in the models used by Murphy et al. (2020).

The prevailing view is that δ Sct pulsations are not found, or are very rare, among Ap stars. As Table A2 shows, this is not the case. *Kepler* observations of TIC 26418690 (KIC 11296437), the star discussed by Murphy et al. (2020), show that it is a δ Sct+roAp star, but the δ Sct peaks have too low an amplitude to be seen in *TESS* data. Murphy et al. (2020) argue that it is not a binary and that the δ Sct and roAp pulsations originate in the same star.

It is interesting to note that the number of δ Sct+roAp stars relative to Ap δ Sct stars (13/199 or about 7 percent), is about the same as the number of δ Sct+roA stars relative to non-Ap δ Sct stars (617/8370 or 7 percent).

To compare the relative number of pulsating Ap/Fp stars with those of normal A/F stars, only main-sequence stars brighter than 10-th magnitude and with $6000 < T_{\text{eff}} < 9000 \text{ K}$ were selected. The magnitude limit ensures that the sample is fairly complete. With these restrictions, there are 37348 stars observed by *TESS* of which 7104 are classified as δ Sct or γ Dor. Thus about 19 percent of all main sequence stars in this temperature range are pulsating δ Sct/ γ Dor variables.

In the same effective temperature and magnitude ranges, there are 875 Ap/Fp stars observed by *TESS* of which 89 are δ Sct or γ Dor stars. Among Ap/Fp stars, about 10 percent pulsate as δ Sct or γ Dor. In the the same T_{eff} and magnitude ranges, there are 60 *TESS* roAp stars. Therefore the fraction of pulsating stars among the chemically peculiar stars is $(89+60)/875$ or about 17 percent. One may conclude that the fraction of pulsating Ap stars is about the same as the fraction of pulsating chemically normal stars. However, there is a very clear tendency for higher frequencies among Ap stars.

Fig. 6 shows the stars listed in Table A2 in the theoretical H-R diagram. It is clear that the chemically peculiar

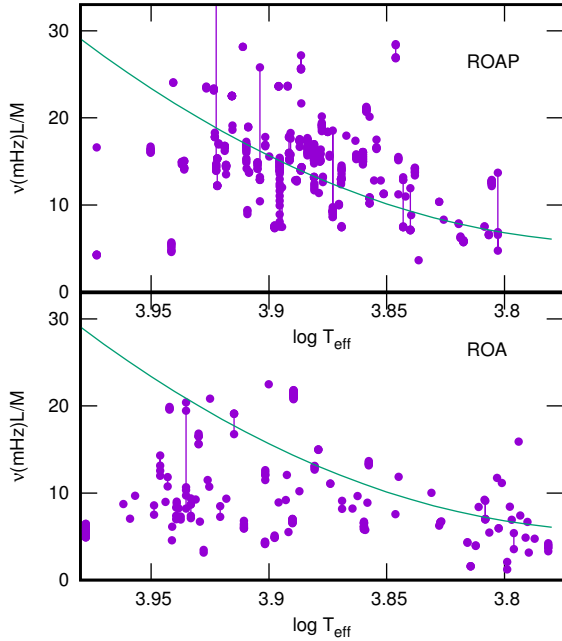


Figure 7. The location of the roAp and roA stars in the $\log T_{\text{eff}} - \nu L/M$ plane where ν is the frequency in mHz and L , M is the luminosity and mass in solar units. Different frequencies in the same star are connected by a vertical line (harmonics ignored). The solid curve is the approximate acoustic critical frequency from models.

δ Sct stars occupy the same instability region as chemically normal δ Sct stars.

9 CRITICAL FREQUENCIES

It has been known for a long time that the pulsation frequencies in a significant number of roAp stars exceed the acoustic critical frequency, ν_{crit} . This is the frequency beyond which the pulsational acoustic waves are no longer reflected in the atmosphere. Modes with $\nu > \nu_{\text{crit}}$ manifest as running waves, leading to energy loss and damping of pulsational driving.

As pointed out by Saio (2014), the critical frequency is best shown in the $\log T_{\text{eff}} - \nu L/M$ plane where ν is the frequency in mHz and L and M are the luminosity and mass in solar units. Fig. 7 shows the location of the roAp and roA stars in this diagram. The calculated critical frequency is adapted from Saio (2014) and Audard et al. (1998). Note that the frequencies in about half the roAp stars exceed the critical acoustic frequency. However, for most of the roA stars the pulsation frequency is below critical.

It is not clear if this result is significant owing to uncertainties in the stellar parameters as well as uncertainties in the atmospheric models used to estimate ν_{crit} . In any case, it is not clear whether the atmospheric structure in highly magnetic stars is the same as in non-magnetic stars. Perhaps the difference can be reconciled in this way and that ν_{crit} is underestimated in the Ap stars. If Ap stars do have systematically higher critical frequencies than normal stars, it might explain why high frequencies are more common among Ap stars.

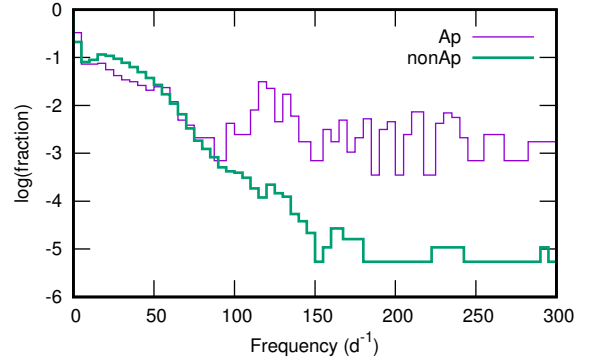


Figure 8. The frequency distribution for δ Sct+ γ Dor+roA stars (thick (green) line) and for Ap δ Sct+ γ Dor+roAp stars (thin violet) line. This is the fraction of independent frequencies within a frequency interval of 5 d^{-1} . All frequency peaks with $S/N > 4.7$ are given the same weight (amplitude ignored).

10 CONCLUSIONS

It is generally believed that chemically peculiar Ap/Fp stars do not pulsate as δ Sct or γ Dor variables. In this paper we have examined 1978 known Ap/Fp stars observed by *TESS* and found that not only do some pulsate as roAp stars, but 199 pulsate as δ Sct or γ Dor stars (Table A2). Furthermore, as Fig. 1 shows, there is no separation in frequency between these chemically peculiar δ Sct stars and the roAp stars. If this were known when the roAp stars were first discovered, there would have been no motivation for creating a separate roAp class at all.

The roAp class, in any case, has never been properly defined. In this paper a hard frequency limit of 60 d^{-1} is used to separate δ Sct from “roAp” stars. This is a purely arbitrary figure. No actual frequency or radial order limit can be established.

The *TESS* observations have shown that isolated high frequencies characteristic of roAp stars can be found in stars which have not been noted as chemically peculiar. In this paper, 103 new stars of this kind are presented (Table A3), in addition to those previously discovered (Cunha et al. 2019; Balona et al. 2019). Some, but not all, of ostensibly non-peculiar stars with isolated frequency peaks in the roAp range have been subsequently found to be chemically peculiar (Holdsworth et al. 2021).

TESS observations of δ Sct stars show that many pulsate with frequencies in the roAp range. The high frequencies in most of these stars are due to combinations or harmonics. An analysis of a large number of δ Sct stars resulted in the discovery of at least 617 high-frequency δ Sct stars with independent pulsation frequencies in the roAp range (Table 3).

All the reasons which motivated the creation of a new class of variable, the roAp stars, have disappeared. It is recommended that the term “roAp” be avoided and that these be considered as normal δ Sct stars. There is no reason to suppose that the high frequencies in normal δ Sct stars are driven by a different mechanism than in the “roAp” stars. The need for the mechanism described by Balmforth et al. (2001) falls away.

The strong magnetic field in Ap stars does, however, affect pulsations in some stars. This is evident in about one-

third of the roAp stars in which equidistant frequency peaks separated by the rotational frequency are seen. It is likely that the strong magnetic field modifies the atmospheric structure so that the sound speed varies in conjunction with the magnetic field over the surface of the star. Under some circumstances, the pulsational amplitude may vary significantly across the surface. This will only be noticeable in the highest frequencies where the pulsational wavelength is comparable with the atmospheric scale height. This explains, in a natural way, why the pulsation axis appears to be aligned with the magnetic axis in some roAp stars (the oblique pulsator model, Kurtz 1982; Kurtz & Shibahashi 1986).

It has been known for some time that the spectroscopic line profile variability in roAp stars is characterized by blue-to-red moving features (e.g. Kochukhov & Ryabchikova 2001a,b). This behaviour is common in many rotating nonradial pulsators and indicates non-axisymmetric pulsations. However, this is inexplicable in the framework of the standard oblique pulsator model of slowly-rotating roAp stars which demands axisymmetric modes. Why only axisymmetric modes seem to be selected is not known. (Kochukhov et al. 2007) suggests that the modes can still be axisymmetric if the line width varies with height in the atmosphere. In the context proposed here, where the pulsation amplitude varies with magnetic field strength because of changes in sound speed, there is no need to assume axisymmetric modes in the oblique pulsator model. Naturally, the pulsation will be magnetohydrodynamic in nature and not purely acoustic.

Saio (2005) and Murphy et al. (2020) discuss pulsation in a model of a star in which convection is suppressed by a strong magnetic field. These calculations predict that high-order g modes typical of γ Dor pulsations are strongly suppressed in Ap stars. In fact, most of the 199 pulsating Ap stars observed by *TESS* are either γ Dor stars (frequencies not exceeding 5 d^{-1}) or contain multiple low frequencies in the γ Dor range if they are δ Sct variables. Evidently, the models of Saio (2005) and Murphy et al. (2020), as they stand, are not supported by observations.

Fig. 8 shows the distribution of extracted frequencies in 12544 non-Ap and 255 pulsating Ap stars. Note that this is not the distribution of stars. Combination frequencies and harmonics have been excluded. It can be seen that in both cases there is a continuous distribution with a long high-frequency tail. The incidence of high frequencies is clearly much higher in “roAp” than in normal δ Sct stars. This does constitute a distinct difference, but it is not directly related to the pulsation mechanism. It would appear that for some reason high frequencies are preferentially selected in stars with strong magnetic fields.

Unfortunately, we have no idea what drives high frequencies in δ Sct stars, both chemically normal and chemically peculiar. As already mentioned, Xiong et al. (2016) have shown that it is possible to drive high frequencies in models of normal intermediate mass stars, but only for stars in a small region of the instability strip. Without a model, further progress in understanding the δ Sct stars cannot be made.

One of the most striking and puzzling results of the *Kepler* and *TESS* missions is that the distribution of frequency peaks in δ Sct stars is completely unpredictable. Two stars with the same effective temperature, luminosity, metallicity

and rotational velocity should have nearly the same observed frequencies. This turns out not to be the case: the frequencies that are observed may be completely different in the two stars (Balona 2021b). It seems that a highly nonlinear mode selection process is active.

There is a further discovery which might impact on the driving of the oscillations. *Kepler* and *TESS* light curves indicate that the light from A and B stars are modulated by rotation (Balona 2019; Balona & Ozuyar 2021). Flares are sometimes seen in A and late B stars (Balona 2012, 2013, 2015, 2021a). At this stage, there is no model which can account for these phenomena in hot stars. It is also possible that accretion of interstellar material may affect the outer layers of A stars, as suggested by Böhm-Vitense (2006).

Current pulsation models assume that the outer layers are static and devoid of magnetic fields. The treatment of the stellar outer layers in current models is therefore incomplete. This may have an impact on the predicted pulsational stability and may play an important role in mode selection. For further progress, it is essential to study the atmospheres of A and B stars in order to understand the nature of the rotational modulation and to detect possible mass motions. Such a study may lead to pulsation models which better reproduce the observations.

DATA AVAILABILITY

The data underlying this article are available in the article.

ACKNOWLEDGMENTS

I thank the National Research Foundation of South Africa for financial support and Dr Gerald Handler for useful comments.

This paper includes data collected by the *TESS* mission. Funding for the *TESS* mission is provided by the NASA Explorer Program. Funding for the *TESS* Asteroseismic Science Operations Centre is provided by the Danish National Research Foundation (Grant agreement no.: DNR106), ESA PRODEX (PEA 4000119301) and Stellar Astrophysics Centre (SAC) at Aarhus University. We thank the *TESS* and TASC/TASOC teams for their support of the present work.

This work has made use of data from the European Space Agency (ESA) mission Gaia (<https://www.cosmos.esa.int/gaia>), processed by the Gaia Data Processing and Analysis Consortium (DPAC, <https://www.cosmos.esa.int/web/gaia/dpac/consortium>). Funding for the DPAC has been provided by national institutions, in particular the institutions participating in the Gaia Multilateral Agreement.

This research has made use of the SIMBAD database, operated at CDS, Strasbourg, France. This research has made use of the VizieR catalogue access tool, CDS, Strasbourg, France (DOI: 10.26093/cds/vizieR). The original description of the VizieR service was published in A&AS 143, 23.

The data presented in this paper were obtained from the Mikulski Archive for Space Telescopes (MAST). STScI is operated by the Association of Universities for Research in Astronomy, Inc., under NASA contract NAS5-2655.

REFERENCES

- Antoci V., Cunha M., Houdek G., et al., 2014, *ApJ*, 796, 118
- Audard N., Kupka F., Morel P., Provost J., Weiss W. W., 1998, *A&A*, 335, 954
- Balmforth N. J., Cunha M. S., Dolez N., Gough D. O., Vauclair S., 2001, *MNRAS*, 323, 362
- Balona L. A., 2012, *MNRAS*, 423, 3420
- , 2013, *MNRAS*, 431, 2240
- , 2014, *MNRAS*, 437, 1476
- , 2015, *MNRAS*, 447, 2714
- , 2018, *MNRAS*, 479, 183
- , 2019, *MNRAS*, 490, 2112
- , 2021a, *Frontiers in Astronomy and Space Sciences*, 8, 32
- , 2021b, *arXiv e-prints*, arXiv:2109.12574
- Balona L. A., Holdsworth D. L., Cunha M. S., 2019, *MNRAS*, 487, 2117
- Balona L. A., Ozuyar D., 2021, *ApJ*, 921, 5
- Baran A. S., Koen C., 2021, *Acta Astron.*, 71, 113
- Baran A. S., Koen C., Pokrzywka B., 2015, *MNRAS*, 448, L16
- Bedding T. R., Murphy S. J., Hey D. R., et al., 2020, *Nature*, 581, 147
- Bertelli G., Girardi L., Marigo P., Nasi E., 2008, *A&A*, 484, 815
- Böhm-Vitense E., 2006, *PASP*, 118, 419
- Bowman D. M., Michielsen M., 2021, *arXiv e-prints*, arXiv:2109.10776
- Breger M., Stich J., Garrido R., et al., 1993, *A&A*, 271, 482
- Cox J. P., 1963, *ApJ*, 138, 487
- Cunha M. S., 2002, *MNRAS*, 333, 47
- Cunha M. S., Alentiev D., Brandão I. M., Perraut K., 2013, *MNRAS*
- Cunha M. S., Antoci V., Holdsworth D. L., et al., 2019, *MNRAS*, 487, 3523
- Dziembowski W., 1977, *Acta Astron.*, 27, 95
- Gaia Collaboration, Brown A. G. A., Vallenari A., Prusti T., de Bruijne J. H. J., Babusiaux C., Bailer-Jones C. A. L., 2018, *ArXiv e-prints*
- Gaia Collaboration, Prusti T., de Bruijne J. H. J., et al., 2016, *A&A*, 595, A1
- Gontcharov G. A., 2017, *Astronomy Letters*, 43, 472
- Holdsworth D. L., Cunha M. S., Kurtz D. W., et al., 2021, *MNRAS*, 506, 1073
- Holdsworth D. L., Smalley B., Gillon M., et al., 2014, *MNRAS*, 439, 2078
- Jenkins J. M., Twicken J. D., McCauliff S., et al., 2016, in *Proc. SPIE*, Vol. 9913, *Software and Cyberinfrastructure for Astronomy IV*, p. 99133E
- Kjeldsen H., Bedding T. R., 1995, *A&A*, 293, 87
- Kochukhov O., Ryabchikova T., 2001a, *A&A*, 377, L22
- , 2001b, *A&A*, 374, 615
- Kochukhov O., Ryabchikova T., Weiss W. W., Landstreet J. D., Lyashko D., 2007, *MNRAS*, 376, 651
- Kurtz D. W., 1978, *Information Bulletin on Variable Stars*, 1436, 1
- , 1982, *MNRAS*, 200, 807
- Kurtz D. W., Shibahashi H., 1986, *MNRAS*, 223, 557
- Michaud G., Charland Y., Vauclair S., Vauclair G., 1976, *ApJ*, 210, 447
- Murphy S. J., Saio H., Takada-Hidai M., Kurtz D. W., Shibahashi H., Takata M., Hey D. R., 2020, *MNRAS*, 498, 4272
- Pecaut M. J., Mamajek E. E., 2013, *ApJS*, 208, 9
- Saio H., 2005, *MNRAS*, 360, 1022
- , 2014, in *IAU Symposium*, Vol. 301, *Precision Asteroseismology*, Guzik J. A., Chaplin W. J., Handler G., Pigulski A., eds., pp. 197–204
- Samus N. N., Kazarovets E. V., Durlevich O. V., Kireeva N. N., Pastukhova E. N., 2017, *Astronomy Reports*, 61, 80
- Skiff B. A., 2014, *VizieR Online Data Catalog*, 1, 2023
- Smalley B., Antoci V., Holdsworth D. L., et al., 2017, *MNRAS*, 465, 2662
- Smalley B., Niemczura E., Murphy S. J., et al., 2015, *MNRAS*, 452, 3334
- Soubiran C., Le Campion J.-F., Brouillet N., Chemin L., 2016, *A&A*, 591, A118
- Stibbs D. W. N., 1950, *MNRAS*, 110, 395
- Wenger M., Ochsenbein F., Egret D., et al., 2000, *A&AS*, 143, 9
- Xiong D. R., Deng L., Zhang C., Wang K., 2016, *MNRAS*, 457, 3163

APPENDIX

Table A1. List of known roAp or roA stars. The TIC number, name, variability type and characteristic pulsation frequency is given, followed by the effective temperature and luminosity. Where available, the rotation period is given. The last column is the spectral type. A colon denotes uncertain values. The variability class is expanded to include the following: r - rotational sidelobes present; s - variable amplitudes and/or frequencies; 2h,3h - highest harmonic present; l - low frequencies present. A row in italics indicates that the star was not observed by *TESS*. The variability type in square brackets means that the high frequencies are not detected in the *TESS* light curve

| TIC | Name | Var Type | ν (d ⁻¹) | T_{eff} (K) | $\log \frac{L}{L_{\odot}}$ (dex) | P_{rot} (d) | Sp Type |
|------------------|--------------------------------|----------------------|-----------------------------|-------------------------|-------------------------------------|-------------------------|----------------------|
| 3814749 | HD 3748 | ROT+ROA | 238.205 | 7945 | 1.05 | 1.689 | A5 |
| 6118924 | HD 116114 | ROAP | 66.461 | 7817 | 1.46 | | F0VpSrCrEu |
| 12968953 | HD 217704 | ROAP | 115.586 | 7669 | 1.28 | | ApSrEuCr* |
| 16596302 | HD 52524 | ROT+ROA: | 74.156 | 8733 | 0.97 | 2.532 | A0 |
| 17676722 | HD 63773 | ACV+ROAP+r | 167.749 | 8754 | 1.27 | 1.599 | ApSrEuCr* |
| 22113439 | TYC 2612-1843-1 | ACV+ROAP | 62.639 | 7900 | 1.38 | 2.119 | A7m: |
| 22132451 | 2MASS J17584421+3458339 | ACV+ROAP | 71.280 | 7700 | 1.14 | 0.860 | A7m: |
| 23671771 | HD 70664 | ROT+ROA | 293.202 | 6223 | 0.90 | 6.135 | F5 |
| 24344701 | HD 34282 | ROA | 75.412 | 9500 | 1.13 | | A0.5Vb(shell) |
| 26418690 | KIC 11296437 | ACV+DSCT+ROAP+r | 121.800 | 7052 | 1.17 | | Ap |
| 26749633 | TYC 3560-2018-1 | [ROAP] | 118.603 | 6898 | 1.17 | | F2V(Sr) |
| 27395746 | KIC 11409673 | ACV+[ROAP]+r | 216.080 | 7490 | 1.04 | 12.214 | Ap |
| 33601621 | HD 42659 | ACV+ROAP+r | 150.990 | 7698 | 1.53 | 2.659 | A3SrCrEu |
| 34783979 | TYC 1787-186-1 | ROA: | 233.958 | 6047 | 0.10 | | |
| 35905913 | HD 132205 | ACV+[ROAP] | 201.658 | 8631 | 1.13 | 7.535 | A2EuSrCr |
| 41259805 | HD 43226 | ACV+ROAP+r | 199.673 | 8721 | 1.25 | 1.714 | ApSrEu(Cr)* |
| 44827786 | HD 150562 | ROAP | 133.661 | 6390 | 1.06 | | A5:EuSi?? |
| 49332521 | HD 119027 | ROAP | 167.790 | 6750 | 1.07 | | ApSrEuCr: |
| 49818005 | HD 19687 | ROAP | 141.860 | 7213 | 1.20 | | FpSrEu(Cr)* |
| <i>58106971</i> | <i>TYC 2269-996-1</i> | <i>DSCT+ROA</i> | <i>79.130</i> | <i>6650</i> | <i>1.09</i> | | <i>A0V</i> |
| 61811148 | TYC 7926-99-1 | DSCT+ACV+ROAP | 164.475 | 7800 | 0.83 | 0.848 | A7m |
| 69855370 | HD 213637 | ROAP | 125.479 | 6414 | 0.78 | | Ap:Eu:Sr:Cr: |
| 71134596 | HD 28548 | DSCT+ROA | 65.245 | 8200 | 1.07 | | A0IV/V λ Boo |
| <i>72428505</i> | <i>HD 195061</i> | <i>DSCT+ROAP</i> | <i>128.860</i> | <i>8000</i> | <i>1.08</i> | | <i>A0Vm</i> |
| 77128654 | HD 97127 | ROAP | 106.618 | 6407 | 0.94 | | F3pSrEu(Cr) |
| 92350273 | CD-33 15279 | ROT+ROA | 244.814 | 7003 | 1.22 | 6.622 | F5 |
| 93522454 | HD 143487 | [ROAP] | 149.472 | 7866 | 1.44 | | A3SrEuCr? |
| 96315731 | HD 51203 | ACV+ROAP | 165.259 | 7693 | 1.06 | 6.674 | ApSrEuCr |
| 96855460 | HD 185256 | ACV:+ROAP | 140.628 | 6646 | 1.10 | 26.329 | ApSrEu:Cr: |
| 98728812 | HD 18407 | ROA | 65.301 | 9159 | 1.31 | | A0V |
| <i>100196783</i> | <i>HD 193756</i> | <i>ROAP</i> | <i>111.024</i> | <i>7545</i> | <i>1.39</i> | | <i>A9SrCrEu</i> |
| 100775380 | HD 39763 | GDOR+ROA | 68.860 | 8420 | 1.4: | | A1V |
| 118247716 | HD 12519 | ROAP | 170.288 | 7403 | 1.00 | | A4pSrEuCr |
| 119327278 | HD 45698 | ACV+ROAP+r | 210.614 | 8445 | 1.23 | 1.085 | A2SrEu |
| 123231021 | KIC 7582608 | GDOR+ACV:+ROAP | 181.699 | 7801 | 1.38 | 9.906 | A7pEuCr |
| 125297016 | HD 69013 | [ROAP] | 128.304 | 6951 | 1.07 | | A2SrEu |
| <i>128821559</i> | <i>TYC 3218-888-2</i> | <i>DSCT+ROAP</i> | <i>75.540</i> | <i>8100</i> | <i>1.07</i> | | <i>A3m</i> |
| 136842396 | HD 9289 | ACV+ROAP+r | 136.953 | 7900 | 1.17 | 8.566 | A3SrEuCr |
| 137797293 | TYC 6390-339-1 | DSCT+ROA | 66.960 | 8200 | 1.13 | | A3 |
| <i>138093523</i> | <i>TYC 3139-1403-1</i> | <i>DSCT+ROA</i> | <i>129.030</i> | <i>7274</i> | <i>0.98</i> | | |
| 139191168 | HD 217522 | ROAP+s | 104.179 | 6834 | 0.92 | | A5SrEuCr |
| 146715928 | HD 92499 | ROAP | 136.703 | 8231 | 1.34 | | A2SrEuCr |
| 152808505 | HD 216641 | GDOR:+ROAP | 119.210 | 6430 | 0.9: | | FpEuCr* |
| <i>153101639</i> | <i>2MASS J16400299-0737293</i> | <i>ACV+ROAP+r+3h</i> | <i>151.891</i> | <i>7500</i> | <i>1.03</i> | <i>3.675</i> | <i>A7VpSrEu(Cr)</i> |
| 156886111 | HD 47284 | ACV+ROAP+r | 112.406 | 8294 | 1.32 | 6.856 | ApSrEuCr* |
| <i>158009180</i> | <i>TYC 5762-828-1</i> | <i>DSCT+ROA</i> | <i>212.660</i> | <i>6000</i> | <i>1.37</i> | | <i>F8</i> |
| 158216369 | KIC 7018170 | ACV+[ROAP]+r | 168.074 | 6927 | 1.12 | 72.747 | Ap |
| 158271090 | TYC 3545-2756-1 | ACV+ROAP+r+2h | 84.033 | 7293 | 1.45 | 5.685 | Ap |
| 158275114 | KIC 8677585 | GDOR+ROAP+2h+s | 136.975 | 7468 | 1.28 | | A5EuCr |
| 159392323 | TYC 3547-2692-1 | ROAP | 128.752 | 6436 | 0.88 | | F3pSrEuCr |
| 163587609 | HD 101065 | ROAP+s | 118.617 | 6246 | 0.91 | | F0?V? pec |
| 167695608 | TYC 8912-1407-1 | ROAP+s | 132.365 | 7292 | 1.34 | | F0pSrEu(Cr) |
| 168383678 | HD 96237 | ACV:+[ROAP] | 103.680 | 8119 | 1.32 | 22.842 | A4SrEuCr |
| 169078762 | HD 225914 | ACV:+[ROAP]+r | 61.448 | 8070 | 1.69 | 5.242 | A5VpSrCrEu |
| 170419024 | HD 151860 | ROAP | 73.452 | 7339 | 1.17 | | ApSrEuCr: |
| 170586794 | HD 107619 | ACV:+ROAP | 152.194 | 6695 | 0.87 | 10.299 | F5pEuCr* |
| 171988782 | HD 258048 | ROAP | 169.537 | 6600 | 0.74 | | F4pEuCr(Sr) |

Table A1 – *continued*

| TIC | Name | Var Type | ν (d ⁻¹) | T_{eff} (K) | $\log \frac{L}{L_{\odot}}$ (dex) | P_{rot} (d) | Sp Type |
|-----------|-------------------------|------------------------|-----------------------------|-------------------------|-------------------------------------|-------------------------|-----------------|
| 173372645 | HD 154708 | ACV+[ROAP] | 180.403 | 6812 | 0.86 | 5.366 | A2SrEuCr |
| 174475885 | HD 61622 | SXARI+ROAP: | 229.188 | 11763 | 2.09 | 0.852 | B9Si |
| 176516923 | HD 38823 | ACV+ROAP | 165.285 | 7551 | 1.13 | 8.572 | A5SrEuCr* |
| 176941102 | HD 106563 | DSCT+ROAP | 65.460 | 8100 | 1.17 | | A3m: |
| 178575480 | HD 55852 | ACV+ROAP: | 207.181 | 8018 | 1.10 | 4.775 | A0SrEuCr |
| 179193226 | HD 122570 | DSCT+ROA | 99.120 | 7550 | 1.42 | | A3/5III: |
| 189996908 | HD 75445 | ROAP | 159.116 | 7364 | 1.26 | | ApSrEuCr: |
| 203817942 | HD 147911 | DSCT+ROAP: | 68.520 | 8200 | 0.78 | | A0V m |
| 206477008 | HD 24426 | GDOR+ROA: | 171.795 | 6765 | 0.54 | | F5V |
| 211404370 | HD 203932 | ACV:+ROAP+r+s | 242.330 | 7350 | 1.23 | 6.419 | A5SrEu |
| 217302172 | HD 156623 | DSCT+ROA | 63.700 | 9040 | 1.21 | | A1V |
| 220073982 | HD 288081 | ROT+ROA+r: | 73.103 | 8832 | 1.41 | 0.307 | A2 |
| 224284872 | TYC 577-322-1 | DSCT+ROA | 60.47 | 9700 | 0.48 | | A3 |
| 237336864 | HD 218495 | ACV+ROAP+r+s | 195.370 | 8120 | 1.02 | 4.200 | A2EuSr |
| 258178726 | BD+25 3139 | DSCT+ROA | 105.120 | 7100 | 1.16 | | F0 |
| 259587315 | HD 30849 | ACV+ROAP+r | 80.444 | 8030 | 1.52 | 15.866 | ApSrCrEu |
| 260751881 | TYC 9131-119-1 | ACV+ROA+2h | 92.753 | 8050 | 1.22 | 1.197 | A5m: |
| 262590112 | TYC 577-322-1 | DSCT+ROA | 60.420 | 8276 | 1.27 | | A5 |
| 264509538 | KIC 10685175 | ACV+ROAP+r | 191.514 | 8179 | 0.96 | 3.103 | Ap |
| 268460597 | HD 52264 | ACV+ROAP: | 192.139 | 10400 | 2.74 | 7.817 | B0Si |
| 268751602 | HD 12932 | ROAP+2h | 124.096 | 7536 | 0.88 | | ApSrEuCr |
| 272598185 | KIC 10483436 | ACV+[ROAP]+r | 116.899 | 7329 | 1.43 | 4.304 | kA5hA7mA9SrCrEu |
| 273777265 | KIC 6631188 | ACV+ROAP+r | 129.038 | 7700 | 1.25 | 2.516 | Ap |
| 279485093 | HD 24712 | ACV+ROAP+r | 235.064 | 7246 | 0.91 | 12.681 | kA5mF0V?Sr |
| 280198016 | HD 83368 | ACV+ROAP+r+4h+s | 123.025 | 7784 | 1.27 | 2.852 | A8VSrCrEu |
| 284377321 | HD 138334 | ROT+ROA | 86.376 | 7869 | 1.32 | 1.523 | A0V |
| 286992225 | TYC 2553-480-1 | ROAP | 235.540 | 7387 | 0.94 | | A9pSrEu |
| 293265536 | TYC 4-562-1 | ROAP | 150.250 | 7300 | 1.39 | | A9pSrEu(Cr) |
| 294266638 | BD-19 2553 | ROT+ROAP | 140.730 | 7212 | 1.05 | | ApSrEu* |
| 294769049 | HD 161423 | ACV+[ROAP] | 195.303 | 8385 | 1.18 | 10.458 | ApSrEu(Cr) |
| 299000970 | HD 176232 | ACV+ROAP | 125.099 | 7775 | 1.41 | 6.050 | A4pSrEuMn |
| 302602874 | TYC 2488-1241-1 | ACV+ROAP+r | 197.262 | 7800 | 1.23 | 3.093 | A6pSrEu |
| 308307808 | CD-60 2021 | DSCT+ROA | 63.293 | 8310 | 1.14 | | A3: |
| 310817678 | HD 88507 | ACV+ROAP+r | 104.136 | 8364 | 1.30 | 2.750 | ApSrEuCr: |
| 315098995 | HD 84041 | ACV+ROAP+s | 95.989 | 7730 | 1.32 | 3.696 | ApSrEuCr |
| 317719322 | HD 40098 | DSCT+ROA | 60.186 | 8990 | 1.23 | | A2/3V |
| 318007796 | HD 190290 | ACV+ROAP+r | 196.330 | 6776 | 1.02 | 4.041 | A0EuSr |
| 322732889 | HD 99563 | ACV+ROAP+r+2h | 134.238 | 9095 | 1.28 | 2.900 | F0Sr |
| 326185137 | HD 6532 | ACV+ROAP+r+2h | 207.032 | 8383 | 1.27 | 1.945 | ApSrCrEu |
| 335303863 | HD 137949 | ACV+ROAP+4h | 174.079 | 8121 | 1.14 | 7.200 | kA9hA5pSrCrEu |
| 340006157 | HD 60435 | ACV+ROAP+r+2h+s | 116.857 | 7860 | 1.27 | 7.679 | A3SrEu |
| 342624968 | HD 207561 | [ROAP:] ⁺ s | 240.000 | 7200 | 1.08 | | F0III m |
| 348717688 | HD 19918 | ROAP+2h+s | 130.475 | 7400 | 1.21 | | ApSrEuCr |
| 349945078 | HD 57040 | ACV+ROAP+r | 183.719 | 8375 | 1.15 | 13.473 | A2EuCr |
| 350146296 | HD 63087 | ACV+ROAP+r | 304.404 | 7753 | 0.96 | 2.664 | F0pEuCr |
| 354619745 | HD 201601 | ACV+ROAP+s | 117.901 | 7588 | 1.18 | 1785.700 | A7pSrCrFe |
| 363716787 | HD 161459 | ACV+ROAP | 119.838 | 6979 | 1.12 | 5.974 | A2EuSrCr |
| 368866492 | HD 166473 | ACV:+ROAP | 163.460 | 7451 | 1.18 | 3.48: | A5SrEuCr |
| 369845536 | UCAC2 13032830 | ACV+ROAP+r | 176.391 | 6900 | 1.25 | 9.529 | F2(p Cr) |
| 371800781 | TYC 9311-73-1 | ACV:+ROAP | 62.540 | 8200 | 1.17 | 0.869 | A4m |
| 375937924 | TYC 525-2319-1 | DSCT+ROAP | 104.860 | 7000 | 1.47 | | A3m: |
| 380651050 | HD 176384 | ROT+ROA | 162.234 | 6490 | 0.98 | 4.184 | F0/2V |
| 380729861 | TYC 297-328-1 | DSCT+ROAP | 68.990 | 7850 | 3.91 | | A4 m |
| 383521659 | HD 137909 | ACV+ROAP | 83.549 | 7997 | 1.59 | 18.487 | kA8hF0pSrCrEu |
| 387115314 | CPD-77 1337 | ROT+ROA | 117.178 | 7679 | 1.15 | 5.264 | A5 |
| 394124612 | HD 218994 | DSCT+ACV+ROAP | 98.870 | 5096 | 1.46 | 11.647 | A3Sr |
| 394272819 | HD 115226 | ACV+ROAP+r | 132.590 | 8916 | 1.27 | 2.989 | ApSrEu: |
| 396749572 | 2MASS J21553126+0849170 | DSCT+ROA | 61.340 | 7915 | 1.67 | | A3 |
| 399665133 | BD+06 763 | ROT+ROA | 71.101 | 8532 | 1.28 | 0.447 | A2 |
| 402546736 | HD 128898 | ACV+ROAP+r | 210.995 | 7463 | 0.81 | 4.480 | A7VpSrCrEu |
| 407661867 | HD 37584 | ROT+ROA | 64.063 | 8656 | 1.22 | 0.562 | A3V |

Table A1 – continued

| TIC | Name | Var Type | ν (d ⁻¹) | T_{eff} (K) | $\log \frac{L}{L_{\odot}}$ (dex) | P_{rot} (d) | Sp Type |
|-----------|-----------------|---------------|-----------------------------|-------------------------|-------------------------------------|-------------------------|------------|
| 407929868 | HD 24355 | ACV+ROAP+r | 224.294 | 8235 | 1.18 | 27.916 | A5VpSrEu |
| 411247704 | HD 196470 | ROAP | 133.402 | 7279 | 1.15 | | A2SrEu |
| 413938178 | HD 148593 | ROAP | 134.784 | 7763 | 1.30 | | A2Sr |
| 420687462 | HD 122970 | ACV+ROAP+s | 129.816 | 6766 | 0.84 | 3.877 | F0CrEuSr |
| 431380369 | HD 20880 | ACV+ROAP+r+s | 74.350 | 8629 | 1.66 | 5.197 | ApSr(EuCr) |
| 432223926 | HD 134214 | ACV+ROAP+2h+s | 254.621 | 7403 | 0.94 | 248.000 | F2VpSrCrEu |
| 434449811 | HD 80316 | ACV+ROAP+r | 194.552 | 8106 | 1.13 | 2.088 | ApSr(Eu?) |
| 439399707 | HD 225186 | ROT+ROA | 60.079 | 7900 | 1.02 | 1.661 | A3V |
| 445543326 | HD 12098 | ACV+ROAP+r | 187.808 | 7152 | 1.10 | 5.460 | F0Eu |
| 465996299 | HD 177765 | ROAP | 60.998 | 7557 | 1.67 | | A5SrEuCr |
| 466260580 | TYC 9087-1516-1 | ROT+ROAP | 115.802 | 6099 | 0.66 | 0.695 | ApEuCr* |
| 468912168 | HD 26400 | DSCT+ROAP | 68.223 | 8150 | 1.15 | | A3m: |
| 469246567 | HD 86181 | ACV+ROAP+r | 232.770 | 7222 | 1.08 | 2.051 | F0Sr |

Table A2. Chemically peculiar stars known to be δ Scuti or γ Doradus variables. The columns are the same as Table A1 (the characteristic frequency is omitted).

| TIC | Name | Var Type | T_{eff} (K) | $\log \frac{L}{L_{\odot}}$ (dex) | P_{rot} (d) | Sp Type |
|-----------|------------------|-----------------|-------------------------|-------------------------------------|-------------------------|-----------------|
| 2849758 | HD 243007 | DSCT | 9033 | 1.99 | | A1Si |
| 3373254 | HD 244248 | DSCT | 7790 | 1.75 | | A5SiSr |
| 3542929 | HD 244372 | DSCT | 8500 | 1.40 | | A1Sr |
| 9211526 | HD 221226 | GDOR | 6840 | 1.12 | | F3Sr? |
| 9668192 | <i>HD 143517</i> | <i>DSCT</i> | <i>9150</i> | <i>1.22</i> | | <i>A3Sr</i> |
| 11646496 | HD 8717 | DSCT+ACV | 7245 | 1.21 | 2.178 | A5pCr |
| 17233245 | HD 27429 | DSCT | 6831 | 0.86 | | F2Vn(Cr) |
| 19924794 | <i>HD 123255</i> | <i>DSCT+ACV</i> | <i>6903</i> | <i>1.27</i> | <i>0.839</i> | <i>F0IV(Cr)</i> |
| 21073591 | BD+29 3448 | DSCT | 7611 | 1.59 | | F0pSr |
| 24693528 | HD 14944 | GDOR | 7522 | 2.20 | | ApEuCr: |
| 26418690 | KIC 11296437 | ACV+DSCT+ROAP+r | 7052 | 1.17 | 7.124 | Ap |
| 27962331 | HD 211074 | DSCTHF | 7939 | 1.11 | | A5pSr(Eu) |
| 29205693 | HD 87679 | DSCT | 7080 | 0.91 | | A9IV(pSr) |
| 30481397 | TYC 8152-1872-1 | DSCT | 7948 | 1.02 | | A2pSrCrEu |
| 30718811 | HD 33043 | GDOR+ACV | 7234 | 1.19 | 0.978 | F0VSr |
| 38136475 | HD 210424 | MAIA | 13062 | 2.56 | | B6Si |
| 31870361 | HD 22488 | DSCT | 7219 | 1.52 | | A3SrEuCr |
| 38586082 | HD 27463 | ACV+DSCT | 8700 | 1.54 | 2.834 | ApEuCrSr: |
| 39818458 | HD 40759 | EA+DSCT | 8785 | 1.94 | | A0CrEu |
| 40564267 | HD 184471 | DSCT | 10000 | 1.85 | | A9SrCrEu |
| 45803944 | HD 42509 | SPB | 10139 | 2.85 | | B9.5VSi: |
| 46041110 | HD 125081 | DSCT | 6803 | 1.41 | | F3SrCrEu |
| 47557667 | <i>HD 129052</i> | <i>DSCT</i> | <i>9400</i> | <i>1.25</i> | | <i>A2SrEu?</i> |
| 48330947 | HD 85766 | DSCT | 7404 | 1.09 | | ApSi:Cr: |
| 49673974 | <i>HD 220556</i> | <i>DSCT</i> | <i>9400</i> | <i>1.27</i> | | <i>A2SrEuCr</i> |
| 50835993 | HD 71434 | DSCT | 7653 | 1.37 | | A2EuCrSi? |
| 57965241 | HD 168314 | DSCT+ACV | 9900 | 1.92 | 7.337 | A0SiEuCr |
| 61004258 | HD 81009 | DSCT | 9164 | 1.63 | | F1pSiSrCrEu |
| 63671517 | HD 53021 | DSCT+ACV | 7650 | 1.94 | 3.757 | B9Si |
| 67467015 | BD+36 363 | GDOR | 6679 | 1.22 | | F3:IVSr: |
| 67668604 | HD 7898 | DSCT | 7312 | 1.11 | | A7pSr |
| 74383341 | HD 244876 | DSCT | 9170 | 1.38 | | A0SiSr |
| 74721794 | HD 245222 | DSCT | 7790 | 1.66 | | A5CrSi |
| 74804951 | HD 245423 | DSCT+ACV | 8260 | 1.41 | 0.667 | A3Si |
| 75242494 | HD 245990 | SPB | 8500 | 1.44 | | A1Si |
| 75421046 | HD 246109 | DSCT | 8260 | 1.63 | | A2Si |
| 75856816 | HD 246685 | DSCT | 6270 | 1.59 | | ASiSr? |
| 76213603 | TYC 1870-1678-1 | DSCT | 9170 | 1.22 | | A0Sr |
| 76294845 | TYC 1866-943-1 | DSCT+ACV | 8500 | 1.42 | 2.841 | A2SiSr |
| 76494115 | HD 81076 | DSCT | 7684 | 1.98 | | A2EuCr? |
| 76532208 | HD 163712 | GDOR | 7852 | 1.65 | | A4Sr |
| 78182769 | HD 82417 | GDOR | 9373 | 2.10 | | A2EuSrCr? |
| 78562609 | HD 50143 | DSCT+ACV | 8384 | 1.40 | 7.453 | B9EuSrCr? |
| 78784187 | HD 249401 | DSCT | 8148 | 1.83 | | A2Si |
| 80152411 | [M67b] +25 513 | DSCT | 9170 | 1.89 | | B9SiSr? |
| 81336388 | TYC 1885-759-1 | GDOR | 9170 | 2.19 | 0.627 | A0Si? |
| 81636104 | HD 252608 | GDOR | 9170 | 1.83 | 0.324 | B9Si |
| 84863628 | HD 45541 | DSCT | 8516 | 1.40 | | A2/3VSi: |
| 88091070 | HD 192969 | DSCT+EB | 8381 | 1.29 | | A5pSi |
| 93550171 | HD 74169 | ACV+GDOR | 9271 | 1.51 | 4.601 | kA0hA2mA7 |
| 97312819 | HD 68351 | SXARI+MAIA | 10833 | 2.78 | 6.536 | A0SiCr* |
| 98660068 | HD 3326 | DSCT | 7439 | 0.93 | | hA5mF0pSr |
| 101444131 | HD 47176 | DSCT | 7746 | 1.11 | | A6VpSr |
| 115559920 | NGC 1960 81 | BCEP+SPB | 16842 | 3.37 | | B9Si |
| 116143102 | HD 245725 | DSCT | 9170 | 2.34 | | A0Si |
| 116247916 | TYC 2408-446-1 | MAIA | 11300 | 2.15 | | B9SiSr |
| 116250519 | HD 245916 | MAIA+SXARI | 11300 | 2.06 | 1.996 | B9SiCrSr |
| 116860722 | HD 246726 | DSCT | 7573 | 1.16 | | A5SiSr |
| 116881415 | HD 3135 | DSCT | 7137 | 1.15 | | F3SiCr |
| 116995376 | TYC 2413-476-1 | DSCT | 9069 | 1.62 | | A0Sr |
| 118114352 | HD 3772 | GDOR | 6789 | 1.06 | | ApSiCr: |
| 118573876 | HD 22128 | DSCT | 6960 | 1.40 | | A9IVpSrEuCrMn |

Table A2 – continued

| TIC | Name | Var Type | T_{eff} (K) | $\log \frac{L}{L_{\odot}}$ (dex) | P_{rot} (d) | Sp Type |
|-----------|-------------------------|----------------|-------------------------|-------------------------------------|-------------------------|-----------------|
| 120598737 | HD 213421 | EA+DSCT | 8716 | 1.80 | | A0Si? |
| 122932611 | HD 134185 | DSCT | 7400 | 1.72 | | F0Si |
| 123231021 | KIC 7582608 | GDOR+ACV:+ROAP | 7801 | 1.38 | 9.906 | A7pEuCr |
| 123587926 | HD 50285 | DSCT+ACV | 9225 | 2.34 | 1.287 | A0Si |
| 127755832 | HD 243356 | DSCT | 9170 | 1.45 | | A0Si |
| 127846482 | HD 243543 | DSCT | 9170 | 1.69 | | A0Sr |
| 127956261 | HD 243526 | DSCT+ACV | 8500 | 1.56 | | A0SiCrSr |
| 127959761 | HD 35436 | DSCT | 8013 | 1.88 | | A1SiSr |
| 130587035 | HD 108506 | DSCT | 7085 | 1.23 | | F2V+n(Cr) |
| 133696007 | HD 67165 | DSCTHF+ACV | 9900 | 1.86 | 0.876 | A0Si |
| 138239074 | BD+41 4078 | DSCT | 7689 | 1.25 | | A5SiCr? |
| 140010384 | HD 72128 | GDOR | 9900 | 2.14 | | A0Si |
| 143168754 | HD 40765 | DSCT | 6767 | 1.50 | | F1SrCrEu |
| 143842651 | HD 65236 | GDOR | 7650 | 2.18 | | B9Si? |
| 144276313 | HD 221760 | DSCTHF+ACV | 8600 | 1.89 | 2.628 | A0VpSrCrEu |
| 145516106 | HD 137732 | ACV+DSCT | 9496 | 2.41 | 3.794 | B9Si |
| 145888834 | HD 76063 | DSCT | 9170 | | | A0Si |
| 145917186 | HD 76141 | DSCT+ACV | 9450 | 1.89 | 2.538 | A0Si |
| 146373520 | HD 91590 | DSCT+ACV | 7900 | 1.33 | 3.314 | ApSi |
| 149037452 | HD 34460 | GDOR | 6441 | | | F3III/IVSr |
| 152086729 | HD 224962 | DSCT | 6768 | 1.52 | | F0Sr |
| 152355010 | HD 156040 | GDOR | 7816 | 1.98 | | B9Si |
| 152808505 | HD 216641 | GDOR:+ROAP | 6430 | 0.93 | | FpEuCr |
| 154714788 | BD+46 3884 | DSCT | 7042 | 1.25 | | F0pCrEu? |
| 155951067 | HD 2202 | GDOR | 6827 | 0.62 | | F0p:Sr: |
| 155966613 | HD 2263 | GDOR | 6997 | 0.94 | | A3II/IIIp:Si: |
| 158484992 | HD 179259 | DSCT | 7604 | 1.00 | | A8EuCr? |
| 158275114 | ILF1 +44 20 | GDOR+ROAP+2h+s | 7468 | 1.28 | | A5EuCr |
| 159647185 | HD 182895 | DSCT | 7068 | 1.61 | | F2CrEu? |
| 160034048 | HD 118214 | GDOR | 9886 | 1.72 | | A1/2pSi |
| 165011138 | HD 200859 | DSCT | 8329 | 2.03 | | A2Si? |
| 166351770 | DM BD+35 4422 | DSCT | 7847 | 1.65 | | A5Si? |
| 169971995 | HD 66533 | DSCT | 9422 | 2.17 | | kB9hA3mA8SrCrEu |
| 177214903 | HD 53854 | ACV+GDOR | 7650 | 2.33 | 0.855 | B9Si |
| 177319683 | HD 223660 | ACV+DSCT | 9000 | 2.16 | 2.821 | B7IIIpSi |
| 178108654 | HD 20476 | DSCTHF | 9176 | 1.96 | | A5Si |
| 178750406 | HD 56206 | ACV+GDOR | 9900 | 2.02 | 4.906 | A0Eu |
| 180894453 | BD+31 3215 | GDOR | 8079 | 1.81 | | ASr? |
| 183668638 | HD 71058 | GDOR | 7416 | 2.08 | | B9EuCrSr? |
| 190682740 | HD 76406 | DSCT+ACV | 8147 | 2.07 | 2.578 | A0Si |
| 191672063 | HD 77809 | DSCT+ACV | 7925 | 1.60 | 4.749 | ApSrCr: |
| 192375956 | BD+46 681 | DSCT | 7681 | 1.69 | | A8VSrCrEuSi |
| 194356599 | HD 653 | ACV+DSCT+ROAP | 10000 | 1.63 | 1.085 | A0CrEu |
| 195449631 | TYC 2700-2295-1 | DSCT | 7116 | 1.95 | | A0Si? |
| 196639668 | HD 156808 | GDOR | 8324 | 3.95 | | A5EuCr |
| 213564899 | HD 338654 | DSCT | 7989 | 1.45 | | A0Si |
| 215818457 | HD 338735 | GDOR | 8593 | 1.21 | | A0Si? |
| 231813751 | HD 38471 | GDOR+ACV | 7650 | 2.08 | 2.429 | B9Si |
| 235568144 | HD 139478 | GDOR | 7184 | 0.80 | | F1Sr? |
| 235676117 | HD 176281 | GDOR | 6850 | 1.16 | | F2pSr: |
| 237564008 | HD 50345 | DSCT | 8833 | 1.63 | | A0EuCr |
| 238659021 | HD 8441 | DSCT | 9471 | 2.34 | | kB8hA3pSrCrEu |
| 239738736 | HD 247232 | DSCT | 9175 | 1.68 | | A2SiCr |
| 239758529 | HD 247437 | GDOR | 7610 | 2.00 | | B9SiSr |
| 239802539 | 2MASS J05482244+3313262 | SXARI+SPB | 11300 | 2.10 | 0.293 | B9SiSr |
| 239833172 | HD 247794 | DSCT | 9170 | 1.69 | | A0Sr |
| 245179731 | HD 191836 | DSCT | 8010 | 1.76 | | A4/5IV/VSr |
| 245641254 | HD 16460 | GDOR | 6393 | 2.48 | | F1IV-VpSrEuCr: |
| 245792896 | HD 28319 | DSCT+E: | 8430 | 1.94 | | A9IVSr |
| 246734602 | HD 174779 | GDOR | 9505 | 2.59 | | ApSiCrSr |
| 248354858 | HD 7133 | DSCT | 7133 | 1.50 | | A3Sr |
| 252906029 | HD 50972 | ACV+DSCT | 9655 | 1.60 | 1.047 | B9VSrCr |

Table A2 – *continued*

| TIC | Name | Var Type | T_{eff} (K) | $\log \frac{L}{L_{\odot}}$ (dex) | P_{rot} (d) | Sp Type |
|-----------|-----------------|---------------|-------------------------|-------------------------------------|-------------------------|-------------------|
| 257921991 | HD 10783 | SXARI+MAIA | 10772 | 1.98 | 4.132 | A2pSiSrCrFe(EuGd) |
| 260204804 | HD 131910 | DSCT | 6966 | 1.59 | | F4EuCr |
| 267021905 | HD 220071 | DSCT+ELL | 7400 | 1.03 | | A7/F0V:p:Si:Sr? |
| 271057422 | HD 75425 | DSCT | 8042 | 1.45 | | A0SrEuCr? |
| 276300910 | HD 134799 | DSCT+ACV+ROAP | 9743 | 1.50 | 7.270 | A7SrCrMg |
| 283613369 | DM BD+35 4340 | DSCT | 7480 | 1.99 | | F0SiSr? |
| 285856246 | HD 243791 | DSCT | 9170 | 1.75 | | A0Sr |
| 289228040 | HD 200177 | DSCT+ACV | 9928 | 1.55 | 1.469 | kA0hA2pCrSr |
| 289410352 | HD 74611 | ACV:+GDOR | 7650 | 2.01 | 7.232 | B9Si |
| 296375471 | HD 131171 | DSCT | 7650 | 2.25 | | B9Si |
| 298197561 | HD 340577 | DSCT | 8461 | 2.22 | | A3SrCrEu |
| 301946105 | HD 7410 | DSCT | 7815 | 1.79 | | A5SrCrEu |
| 303478699 | HD 154253 | DSCT+ACV | 8001 | 1.52 | 3.094 | A0SrCrEu |
| 307642246 | HD 72634 | ACV+DSCT | 9300 | 1.96 | 1.861 | A0EuCrSr |
| 307930890 | HD 85672 | DSCT+ROAP | 7850 | 0.99 | | A3VpSr |
| 310295579 | HD 107267 | DSCT | 9951 | 2.17 | | B8Si |
| 311778802 | HD 39135 | DSCT | 8645 | 2.31 | | A0SiCrSr |
| 311911447 | TYC 2410-948-1 | DSCT | 10571 | 1.95 | | A0Sr? |
| 312221714 | HD 248727 | DSCT | 9790 | 1.89 | | A0MnSiCr |
| 312690491 | DM BD+34 1215 | MAIA | 11300 | 1.98 | | B9Si? |
| 316520410 | HD 21427 | GDOR | 9078 | 1.54 | | A3VSi: |
| 318717035 | HD 3992 | DSCT | 8500 | 1.97 | | A3pSi |
| 320504339 | HD 2852 | DSCT | 7835 | 1.92 | | A5SrEu |
| 323432344 | HD 32314 | DSCT | 8044 | 1.07 | | A5Si |
| 324437240 | HD 169594 | DSCT+ACV | 8328 | 1.94 | 1.649 | ApCrSrSi |
| 331644554 | DM BD+46 3543 | EA+DSCT | 8450 | 1.17 | | A2Si |
| 333808016 | HD 62632 | DSCT+ACV | 8810 | 2.05 | 3.281 | A2CrEu |
| 341616734 | HD 89069 | GDOR | 8941 | 1.65 | | A0SrCrEu* |
| 342575976 | HD 170005 | DSCT | 7785 | 1.59 | | A2pSr |
| 343126267 | BD+54 2730 | DSCT | 7998 | 1.12 | | F0SiSr |
| 344177424 | HD 89877 | DSCT+ACV | 8925 | 2.41 | 3.186 | ApEuCrSr: |
| 345426423 | TYC 4004-312-1 | GDOR | 8217 | 1.46 | | A0Si? |
| 348772511 | HD 21190 | DSCT | 7028 | 1.62 | | F2IIISrEuSi: |
| 353436357 | HD 47774 | DSCT+ACV | 9170 | 2.41 | 2.849 | A0III-IVCrEu |
| 356088697 | HD 76460 | DSCT | 8454 | 1.52 | | ApSrEuCr* |
| 356439350 | HD 181331 | DSCT+ACV | 9900 | 2.22 | 3.571 | A0VpSi |
| 361168660 | HD 144059 | EA+DSCT | 9900 | 2.37 | | A0III: |
| 362622494 | HD 147174 | DSCTHF | 9900 | 1.72 | | A0SiCrSr |
| 363387100 | HD 192060 | GDOR | 7140 | 1.51 | | A5YSr? |
| 363550117 | HD 99458 | EB+DSCT | 7600 | 1.57 | | A2 |
| 364257619 | HD 191426 | DSCT+ACV | 9900 | 3.55 | 3.184 | A0Si |
| 369711187 | HD 47633 | ACV+GDOR | 9174 | 1.77 | 6.041 | B9Si |
| 371976932 | HD 240242 | DSCT | 9400 | 1.06 | | A4Si |
| 382538797 | HD 145393 | DSCT | 7015 | 1.05 | | A9Vp:Eu:Cr:Sr: |
| 382631655 | CPD-60 922 | DSCT+ACV | 7295 | 0.91 | 1.446 | A0Si? |
| 385594939 | [M67b]+23 477 | DSCT | 9400 | 0.84 | | kA2mF0SrSi |
| 389841228 | BD+38 2360 | GDOR | 7042 | 0.88 | | F0pSrCrEu |
| 393799555 | HD 108283 | DSCT+ACV | 7170 | 1.84 | 1.272 | A9IVnpSr |
| 394124612 | HD 218994 | DSCT+ACV+ROAP | 5096 | 1.46 | 11.647 | A3Sr |
| 401529004 | HD 77830 | DSCT | 7821 | 1.66 | | A5SrCr |
| 408246457 | HD 281886 | GDOR | 6547 | 0.64 | | F0pSr? |
| 410163387 | HD 76276 | GDOR+ROAP | 7697 | 1.52 | | A0SrCrEu |
| 417206015 | HD 205171 | DSCT | 9888 | 1.67 | | kA0.5mA1Vas(Si) |
| 418241480 | HD 19978 | DSCT | 7780 | 1.59 | | ApCrEuSr |
| 419916333 | HD 117290 | DSCT | 7271 | 1.77 | | A3EuCrSr |
| 420656936 | HD 4853 | DSCT+ACV | 8536 | 1.56 | 0.579 | A3Si |
| 426009799 | HD 139855 | GDOR | 7609 | 1.53 | | A0Si |
| 427377135 | HD 36955 | DSCTHF+ACV | 8057 | 1.63 | 2.283 | kA0hA2mA4CrEu |
| 429306233 | HD 97411 | DSCT+ROA | 10000 | 1.79 | | A0p(Si) |
| 429501634 | HD 40724 | SPB | 11677 | 2.50 | | B8VSiCr |
| 429553764 | HD 40696 | GDOR | 8187 | 2.12 | | A0Si? |
| 429556532 | TYC 1864-1509-1 | GDOR | 7555 | 1.94 | | A2pSr: |
| 431029903 | TYC 3982-4172-1 | DSCT | 7276 | 1.53 | | A3pSr |
| 435263600 | HD 218439 | GDOR+ROAP | 8283 | 1.91 | 3.120 | A2p:Sr:Cr:Si: |

Table A2 – continued

| TIC | Name | Var Type | T_{eff} (K) | $\log \frac{L}{L_{\odot}}$ (dex) | P_{rot} (d) | Sp Type |
|-----------|-----------|-------------|-------------------------|-------------------------------------|-------------------------|---------------|
| 437231105 | HD 95158 | DSCT | 7193 | 1.40 | | A7SrCr? |
| 438694338 | HD 117227 | DSCTHF | 7803 | 1.07 | | A0CrSr |
| 445325141 | HD 59660 | DSCT+ACV | 8251 | 2.30 | 4.283 | A0EuCr? |
| 445796153 | HD 34740 | ACV:+DSCTHF | 7351 | 1.16 | 5.576 | A0pSrSi |
| 449026092 | HD 125467 | DSCT+ACV | 8000 | 1.68 | 3.891 | ApEuCrSr |
| 450091404 | HD 287150 | DSCT | 8169 | 1.72 | | A3SrCr? |
| 452907921 | HD 66853 | DSCT: | 7120 | 1.38 | | F2IIIpSrEuCr: |
| 454802988 | HD 133792 | GDOR | 9900 | 2.22 | | A0pSrCrSi |
| 464254336 | HD 90178 | GDOR | 9900 | 2.11 | | A0Si |
| 470215950 | HD 161704 | DSCT | 6408 | 0.57 | | Ap:Cr:Eu:Sr: |
| 470680611 | HD 195147 | DSCT | 6889 | 1.39 | | F0pSrSi |

Table A3. List of new roAp and roA stars. The columns are the same as in Table A1. A colon on the variable type signifies stars with a signal-to-noise ratio $S/N < 5$.

| TIC | Name | Var Type | ν (d ⁻¹) | T_{eff} (K) | $\log \frac{L}{L_{\odot}}$ (dex) | P_{rot} (d) | Sp Type |
|-----------|-----------------|---------------|-----------------------------|-------------------------|-------------------------------------|-------------------------|------------|
| 4463975 | TYC 5820-1216-1 | ROA+ROT | 174.753 | 7629 | 1.05 | 0.514 | F0 |
| 5370150 | HD 55133 | ROT+ROA: | 226.528 | 6927 | 0.45 | 3.663 | F6/8(IV) |
| 7647538 | HD 27440 | ROT+ROA: | 248.231 | 6497 | 1.06 | 6.024 | F5IV/V |
| 9171107 | TYC 2479-429-1 | ROT+ROA | 132.107 | 6523 | 0.1: | 3.096 | |
| 12312526 | HD 291240 | ROA | 66.213 | 8249 | 1.11 | | A2 |
| 21024812 | HD 14522 | ACV+ROAP | 95.265 | 7942 | 1.46 | 13.158 | A8VSrEuSi |
| 25676603 | BD+27 4042 | ACV+ROAP | 157.205 | 6568 | 0.86 | 5.495 | F0SrEu |
| 26833276 | HD 10682 | ACV+ROAP | 136.786 | 6967 | 0.80 | 10.417 | F0VpSr |
| 27011098 | KIC 10925227 | ROT+ROA | 199.341 | 7532 | 1.00 | 3.247 | |
| 30965889 | CPD-44 3294 | ROA | 60.968 | 8773 | 1.18 | | A0 |
| 31148852 | CD-46 4837 | ROA | 61.011 | 8587 | 1.14 | | A2V |
| 33416333 | HD 217249 | ROA+ROT | 238.461 | 6891 | 1.02 | 4.831 | A7III |
| 33604636 | HD 42605 | ACV+ROAP | 108.633 | 8283 | 1.37 | 2.778 | ApSrEuCr |
| 36576010 | HD 216018 | ROAP | 166.682 | 8400 | 1.24 | | A9VpSrCrEu |
| 40485583 | HD 227470 | ROA | 62.560 | 7501 | 1.20 | | A1V |
| 43135807 | HD 116856 | ROA | 78.231 | 5951 | 0.67 | | G0III |
| 48188257 | KIC 11175495 | EA+ROA | 64.434 | 8554 | 1.36 | | |
| 50656687 | HD 36117 | ROT+ROA: | 86.170 | 7655 | 1.30 | 1.484 | A2Va |
| 68191357 | HD 172585 | ROA+ROT | 63.018 | 8740 | 1.31 | 5.917 | F |
| 68343162 | TYC 2637-1765-1 | ROT+ROA | 150.802 | 6238 | 0.11 | 5.495 | |
| 68972304 | HD 231442 | ROA | 62.659 | 7059 | 1.66 | | A2 |
| 71148851 | HD 233534 | ROA+ROT | 65.543 | 7762 | 1.17 | 2.967 | A2 |
| 72392575 | HD 225578 | ACV+ROAP | 135.944 | 7828 | 1.07 | 3.922 | A5Sr? |
| 80542072 | HD 67804 | ROT+ROA+FLARE | 62.978 | 6176 | 1.15 | 1.634 | A2/3IV |
| 89757305 | HD 227658 | SPB+ROA | 288.146 | 21838 | 3.42 | | B2 |
| 91224991 | HD 191380 | ROA+2h | 100.213 | 6958 | 0.96 | | F8 |
| 93270207 | HD 73904 | ROA | 79.244 | 9229 | 1.29 | | A2VhA0?n |
| 96329159 | HD 146313 | ROT+ROA: | 107.053 | 6575 | 0.92 | 1.420 | F2V |
| 101403577 | HD 189609 | ROT+ROA | 64.367 | 5672 | 1.03 | 2.079 | A1V |
| 101624823 | HD 100598 | ROT+ROA | 124.568 | 6859 | 1.08 | 4.049 | F0 |
| 115642252 | NGC 1960 109 | BCEP+ROA | 60.991 | 7212 | 2.45 | | B2I |
| 120532285 | HD 213258 | ROA | 192.349 | 7871 | 0.96 | | Fp |
| 120663727 | HD 49832 | ROA | 67.249 | 8754 | 1.24 | | A1V |
| 127944540 | HD 127592 | ROA | 217.182 | 6919 | 1.18 | | A8/9V GAIA |
| 129820552 | BD+36 467 | ACV+ROAP | 173.928 | 7742 | 0.97 | 6.211 | ApSrEu |
| 132923245 | CD-41 3649 | ROA+FLARE | 78.000 | 8124 | 1.25 | | B9 |
| 134361875 | HD 55450 | ROA | 72.861 | 8454 | 1.22 | | A0V |
| 134860590 | HD 68625 | ROA+ROT | 61.326 | 9002 | 1.22 | 3.861 | A2V |
| 143400338 | BD-03 2896 | ROA: | 167.650 | 6253 | 0.74 | | F0: |
| 146440176 | HD 32488 | ROA: | 71.377 | 6660 | 1.03 | | F3/5V |
| 148899733 | HD 137015 | ROA+ROT | 80.805 | 8879 | 2.35 | 0.763 | A1/2V GAIA |
| 152896524 | HD 156120 | ROT+ROA+r | 144.975 | 7906 | 1.22 | 5.587 | A7/9V: |
| 156810780 | HD 51093 | ROA | 61.667 | 9097 | 1.25 | | A1V |
| 157542967 | HD 171945 | ROT+ROA+r | 61.051 | 9072 | 1.38 | 0.384 | A2 |
| 159195919 | HD 128360 | ROA+ROT | 64.081 | 7240 | 1.13 | 1.669 | A1V |
| 165052884 | HD 51561 | ROT+ROA | 188.069 | 7711 | 0.84 | 17.857 | A5 |
| 172356142 | HD 46399 | ROT+ROA | 61.024 | 6047 | 1.04 | 2.004 | A2V |
| 173082020 | HD 104366 | ROA | 67.910 | 8178 | 0.94 | | A3Vp |
| 185163987 | HD 72916 | ROT+ROA | 63.706 | 8731 | 1.17 | 10.989 | A3V |
| 192970685 | HD 67871 | ROT+ROA | 61.222 | 7868 | 1.34 | 0.731 | A2V |
| 193808452 | BD+42 3743 | ROA: | 224.721 | 7227 | 3.39 | | A2II |
| 194356599 | HD 653 | ACV+DSCT+ROAP | 61.102 | 10000 | 1.63 | 1.085 | A0CrEu |
| 198107724 | HD 121825 | ROA: | 183.429 | 5796 | 0.17 | | F9V |
| 206481548 | HD 209719 | ROT+ROA | 62.860 | 8007 | 1.13 | 1.125 | A1IV/V |
| 231277305 | HD 17703 | ROA: | 124.867 | 6298 | 0.63 | | F6V |
| 231953659 | TYC 8106-673-1 | ROA | 81.132 | 6080 | 0.49 | | |
| 233200244 | HD 161846 | ROT+ROA+r | 124.471 | 8930 | 1.38 | 7.299 | A3 |
| 233398254 | HD 191490 | ROT+ROA | 83.931 | 8734 | 1.27 | 3.049 | A2 |
| 242198772 | HD 294848 | ROT+ROA+r | 202.346 | 8544 | 1.16 | 1.616 | A7 |
| 244991415 | HD 339572 | ROA+ROT | 206.463 | 7906 | 1.25 | 8.065 | A7 |
| 246937824 | HD 14126 | ROA | 173.131 | 7461 | 0.98 | | A2 |

Table A3 – continued

| TIC | Name | Var Type | ν (d^{-1}) | T_{eff} (K) | $\log \frac{L}{L_{\odot}}$ (dex) | P_{rot} (d) | Sp Type |
|-----------|-------------------------|--------------------|------------------------------|-------------------------|-------------------------------------|-------------------------|---------------|
| 249648704 | HD 215449 | ROT+ROA: | 103.634 | 8223 | 1.04 | 4.405 | A7III |
| 255988376 | HD 158952 | ROT+ROA | 73.386 | 9180 | 1.23 | 12.500 | A0V |
| 257168451 | BD+00 2086 | ROA | 63.038 | 8501 | 1.12 | | A2 |
| 258626846 | TYC 4451-487-1 | ROT+ROA | 61.364 | 7522 | 0.96 | 3.584 | |
| 259017938 | HD 210684 | ROT+ROA+r | 116.825 | 7770 | 1.31 | 5.102 | F0 |
| 259019958 | HD 130232 | ROA | 80.703 | 8210 | 1.14 | | A0V |
| 261191518 | HD 155945 | ROT+ROA | 144.732 | 6774 | 1.11 | 0.777 | F0V |
| 265886274 | HD 347793 | ROA | 71.767 | 8214 | 1.26 | | A0 |
| 266806814 | HD 62526 | ROT+ROA | 190.441 | 8681 | 1.19 | 12.821 | A0 |
| 274644686 | HD 227534 | BCEP+ROA | 67.054 | 18950 | 1.85 | | B5:V: |
| 276300910 | HD 134799 | DSCT+ACV+ROAP | 65.304 | 9743 | 1.50 | 7.270 | F0IIISrCrMg |
| 282086296 | HD 311505 | ROT+ROA: | 277.490 | 6662 | 0.35 | 4.082 | G0 |
| 287636619 | TYC 9201-1206-1 | ROA: | 243.548 | 6472 | 0.57 | | |
| 288242217 | HD 158012 | ROT+ROA | 69.212 | 7480 | 1.53 | 5.051 | F0 |
| 293290586 | HD 129842 | ROT+ROA | 156.888 | 13520 | 2.83 | 0.672 | B8/9IV/V |
| 295254609 | HD 163362 | ROT+ROA | 74.176 | 8548 | 1.24 | 166.667 | A2V |
| 298052991 | BD+78 451 | ROT+ROA | 197.951 | 7680 | 0.92 | 10.638 | A2 |
| 299467756 | HD 294788 | ROT+ROA | 81.352 | 8758 | 1.74 | 1.733 | A0V |
| 304425262 | HD 103079 | SPB+BCEP+ROA | 61.337 | 20560 | 3.02 | | B4IV |
| 306090385 | HD 344856 | ROT+ROA | 63.180 | 8909 | 1.24 | 4.926 | A0 |
| 306250556 | HD 301370 | ROT+ROA | 204.338 | 7494 | 1.17 | 4.651 | A3 |
| 307606851 | HD 135344 | ROA | 79.938 | 9055 | 1.20 | | A0V |
| 307930890 | HD 85672 | DSCT+ROAP | 65.363 | 7850 | 0.99 | | A3VpSr |
| 308085294 | HD 74388 | ACV+ROAP: | 179.185 | 7654 | 2.39 | 4.323 | B8Si |
| 308752235 | TYC 8932-623-1 | ROT+ROA: | 78.805 | 6109 | -0.01 | 8.000 | |
| 313261813 | HD 119476 | GDOR+ROT+ROA | 79.115 | 9058 | 1.32 | 0.442 | A1.5V |
| 319740524 | HD 182396 | ROT+ROA | 70.022 | 8673 | 1.2: | 2.890 | A2V |
| 335457083 | HD 48409 | ROT+ROA+r | 180.075 | 8510 | 1.10 | 2.907 | A3 |
| 349071261 | HD 284113 | EP+ROA | 101.213 | 6381 | 0.54 | | F8 |
| 352787151 | BD+35 5094 | ROAP | 60.138 | 7034 | 1.55 | | F0SrEu |
| 355281777 | HD 56663 | ROT+ROA | 68.121 | 8887 | 1.22 | 4.149 | A1/2V |
| 358289524 | HD 26564 | ROA | 63.282 | 8690 | 1.31 | | A1V |
| 358464975 | CPD-60 933 | ROA+GDOR | 66.671 | 8675 | 1.22 | | A2 |
| 359030908 | HD 104956 | ROA | 206.915 | 6125 | 0.34 | | F8 |
| 360020620 | HD 190833 | GDOR+ROT+FLARE+ROA | 64.928 | 7406 | 1.26 | 0.568 | A0V |
| 362351038 | HD 140498 | ROA | 70.091 | 8266 | 1.19 | | A0V |
| 366554105 | HD 210695 | ROT+ROA: | 97.151 | 6972 | 1.05 | 0.806 | F5 |
| 376942777 | HD 274350 | ROA | 81.453 | 6733 | 1.01 | | F2 |
| 380584567 | BD+12 2366 | ROA: | 115.405 | 6243 | 0.78 | | F8 |
| 383657251 | HD 77422 | ROA+ROT | 62.325 | 8760 | 1.14 | 1.603 | A3V |
| 383704522 | HD 129912 | ROA: | 203.033 | 6659 | 0.68 | | F3V |
| 385939181 | HD 302131 | ROT+ROA | 60.737 | 9317 | 1.22 | 4.785 | A2 |
| 389879483 | HD 100474 | ROA: | 82.936 | 6420 | 1.03 | | F5V |
| 392924760 | HD 120200 | GDOR+ROA: | 198.147 | 7211 | 0.90 | | A5 |
| 394860395 | BD+35 3616 | ACV+ROAP | 101.949 | 11007 | 1.36 | 6.667 | F0SrEu |
| 398476730 | HD 104125 | ROT+ROA | 69.088 | 8656 | 1.35 | 1.280 | A2V |
| 405892692 | BD+49 3179 | ROT+ROA | 101.159 | 7527 | 0.85 | 0.383 | F0 |
| 411923607 | CD-63 1324 | ROA | 101.793 | 6232 | 0.21 | | |
| 423315454 | 2MASS J23293590+1022092 | ROA+ROT | 63.379 | 8086 | 1.46 | 1.387 | A1 |
| 427398460 | HD 294239 | ROA | 83.515 | 8772 | 1.22 | | B5 |
| 427400331 | HD 290662 | ACV+ROAP | 75.050 | 7418 | 0.70 | 0.943 | A0Vp |
| 435263600 | HD 218439 | GDOR+ACV+ROAP | 94.796 | 8283 | 1.91 | 3.106 | A2p:Sr:Cr:Si: |
| 442896389 | HD 34995 | ROT+ROA | 174.274 | 6717 | 0.61 | 3.759 | F2V |
| 444006544 | HD 74911 | GDOR+ROA | 63.549 | 7950 | 1.50 | | A2IV |
| 445493624 | HD 11948 | ACV+ROAP: | 105.857 | 8344 | 1.41 | 7.333 | A5SrEu |
| 450851808 | HD 98435 | ROT+ROA | 63.945 | 7394 | 1.31 | 2.976 | A1/2V |
| 453826702 | HD 22032 | ACV+ROAP+r | 139.102 | 7601 | 1.21 | 4.854 | A3SrEuCr |
| 456673854 | HD 59702 | ACV+ROAP+r | 273.822 | 8100 | 1.04 | 5.435 | A7pSrEu |
| 464740586 | HD 302881 | ROA | 67.454 | 8511 | 1.12 | | A2 |
| 464807201 | HD 29839 | ROA+ROT | 78.447 | 7956 | 1.65 | 5.682 | A1V |
| 630844439 | HD 10581 | GDOR+ACV+ROAP | 289.721 | 7018 | 1.14 | 1.664 | A8m |